3

Harmonic Sources

3.1 Introduction

Prior to the appearance of power semiconductors, the main sources of waveform distortion were electric arc furnaces, the accumulated effect of fluorescent lamps, and to a lesser extent electrical machines and transformers.

The increasing use of power electronic devices for the control of power apparatus and systems has been the reason for the greater concern about waveform distortion in recent times. A power electronic converter can be viewed as a matrix of static switches that provides a flexible interconnection between input and output nodes of an electrical power system. Through these switches power can be transferred between input and output systems operating at the same or different frequencies (one or both of which can be d.c.).

The most common power electronic aid is the single-phase rectifier, used to power most modern office and domestic appliances. Although the individual ratings are always small, their combined effect can be an important source of waveform distortion.

Because of their considerable power ratings, three-phase static power converters are the main contributors to the harmonic problem. The terms *rectification* and *inversion* are used for power transfers from a.c. to d.c. or d.c. to a.c., respectively and the term *conversion* is used when the power electronic device has bi-directional power transfer capability.

According to the relative position of the firing instant of the switches from one cycle to the next on the steady state, four basically different power electronic control principles are in common use:

(1) Constant phase-angle control produces consecutive valve firings equally spaced with reference to their respective commutating voltages.

(2) Equidistant firing control produces consecutive firings at equal intervals of the supply frequency.

(3) Modulated phase-angle control produces time-varying phase-modulated firings.

(4) Integral cycle control selects an integer number of complete cycles or half cycles of the supply frequency.

Power System Harmonics, Second Edition J. Arrillaga, N.R. Watson
 ISBN: 0-470-85129-5

The Fourier analysis as described in Chapter 2 is directly applicable to the phase-angle controlled and equidistant-firing controlled waveforms, whereas modulated firing and integral cycle controls require special analysis.

Inverter fed a.c. drives are normally supplied from the a.c. power system through a line-commutated three-phase rectifier and thus their harmonic contribution to the power network is covered under the various static converter categories. However, the inverter side of the drive uses either pulse width modulation (PWM) and/or multi-level configurations to reduce the harmonic content and, thus requires special consideration.

3.2 Transformer Magnetisation Nonlinearities

3.2.1 Normal Excitation Characteristics

At no-load the primary of a transformer is practically balanced by the back e.m.f. because the effect of winding resistance and leakage reactance is negligible at low currents. At any instant, therefore, the impressed voltage v_1 for a sinusoidal supply is

$$v_1 = -e_1 = -E_m \sin \omega t = N_1 \frac{\mathrm{d}\phi}{\mathrm{d}t} \tag{3.1}$$

From equation (3.1) the following expression is obtained for the main flux:

$$\phi = -\int \frac{e_1}{N_1} \mathrm{d}t = \frac{E_m}{N_1 \omega} \cos \omega t = \phi_m \cos \omega t \tag{3.2}$$

i.e. a sinusoidal primary voltage produces a sinusoidal flux at no-load. The primary current, however, will not be purely sinusoidal, because the flux is not linearly proportional to the magnetising current, as explained in the next section.

3.2.2 Determination of the Current Waveshape

In an ideal core without hysteresis loss the flux ϕ and the magnetising current needed to produce it are related to each other by the magnetising curve of the steel used in the laminations, as shown in Figure 3.1(a). In Figure 3.1(b), where ϕ represents the sinusoidal flux needed to balance the primary voltage, the magnetising current is plotted against time for each value of ϕ and the resulting waveform is far from sinusoidal. However, when operating at or close to the nominal voltage, the transformer magnetising current is only 1–2% of the rated current and presents no special problem.

When the hysteresis effect is included, as in the case of Figure 3.2, the non-sinusoidal magnetising current wave is no longer symmetrical about its maximum value. In this case the current corresponding to any point on the flux density wave of Figure 3.2(b) is determined from Figure 3.2(a), the ascending portion of the hysteresis being used for the ascending portion of the flux density wave.

The distortion illustrated in Figures 3.1 and 3.2 is mainly caused by zero-sequence triplen harmonics and particularly the third. Thus, in order to maintain a reasonably

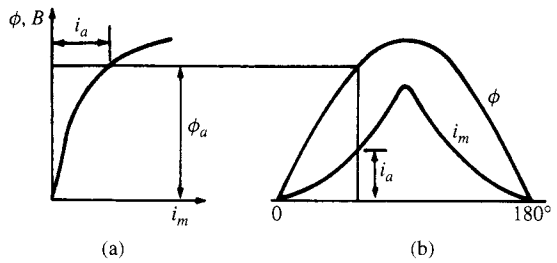

Figure 3.1 Transformer magnetisation (without hysteresis): (a) magnetisation curve; (b) flux and magnetisation current waveforms

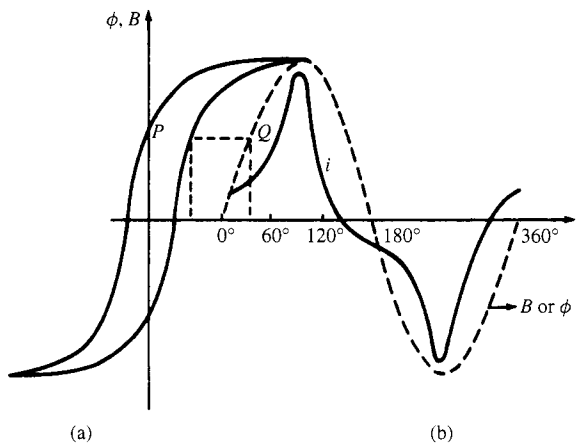

Figure 3.2 Transformer magnetisation (including hysteresis): (a) magnetisation curve; (b) flux and magnetisation current waveforms

sinusoidal voltage supply, it is necessary to provide a path for the zero-sequence current harmonics and this is normally achieved by the use of delta-connected windings.

With three-limb transformers the triplen harmonic m.m.f.s are all in phase and they act in each limb in the same direction. Hence the path of triplen harmonic flux must return through the air (or rather through the oil and transformer tank) and the higher reluctance of such a path reduces the triplen harmonic flux to a very small value (about 10% of that appearing in independent core phases). Thus, flux density and e.m.f. waveforms remain sinusoidal under all conditions in this case. However, the elimination of triplen harmonics in the delta-connected windings is only fully effective when the voltages are perfectly balanced. The magnetising current harmonics often rise to their maximum levels in the early hours of the morning, i.e. when the system is lightly loaded and the voltage high.

3.2.3 Symmetrical Overexcitation

For economic reasons transformers are normally designed to make good use of the magnetic properties of the core material. This means that a typical transformer using a

good quality grain-oriented steel might be expected to run with a peak magnetic flux density in the steady state of the order of 1.6–1.7 T. If a transformer running with this peak operating magnetic flux density is subjected to a 30% rise in voltage, the core material may be subjected to a magnetic flux density of, say, 1.9–2.0 T, which will produce considerable saturation.

The problem of overvoltage saturation is particularly onerous in the case of transformers connected to large rectifier plant following load rejection. It has been shown [1] that the voltage at the converter terminals can reach a level of 1.43 per unit, thus driving the converter transformer deep into saturation.

The symmetrical magnetising current associated with a single transformer core saturation contains all the odd harmonics. If the fundamental component is ignored, and if it is assumed that all triplen harmonics are absorbed in delta windings, then the harmonics being generated are of orders 5, 7, 11, 13, 17, 19 ..., i.e. those of orders $6k \pm 1$, where k is an integer. In conventional six-pulse rectifier schemes it is usual to filter these harmonics from the a.c. busbars as they are exactly of the same order as the theoretical harmonics produced by a six-pulse converter. If, however, a twelve-pulse converter configuration is used, the theoretical harmonics are of orders $12k \pm 1$, where k is an integer. In this case the fifth- and seventh-order harmonics produced by a saturated converter transformer are not filtered and have to be absorbed by the a.c. system.

The composition of the magnetising current versus the exciting voltage is typically as shown in Figure 3.3.

3.2.4 Inrush Current Harmonics

If a transformer is switched off it can be left with a residual flux density in the core of magnitude $+B_r$ or $-B_r$ (or under some circumstances zero). When the transformer is re-energised the flux density illustrated in Figure 3.4 can reach peak levels of $2B_{max}$ or

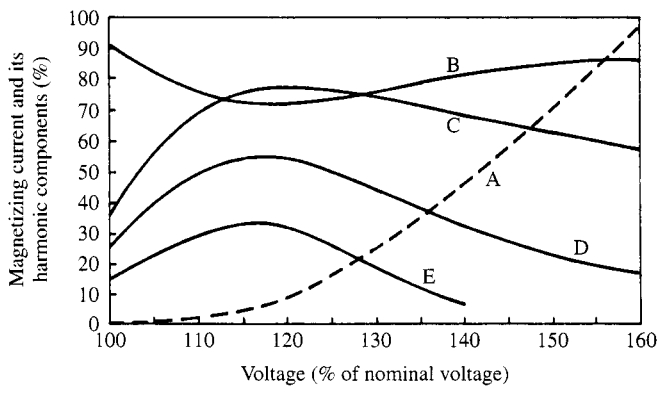

Figure 3.3 Harmonic components of transformer exciting current: A, magnetising current (% of rated current); B, fundamental component (% of total magnetising current); C, third harmonic (% of fundamental current); D, fifth harmonic (% of fundamental current); E, seventh harmonic (% of fundamental current)

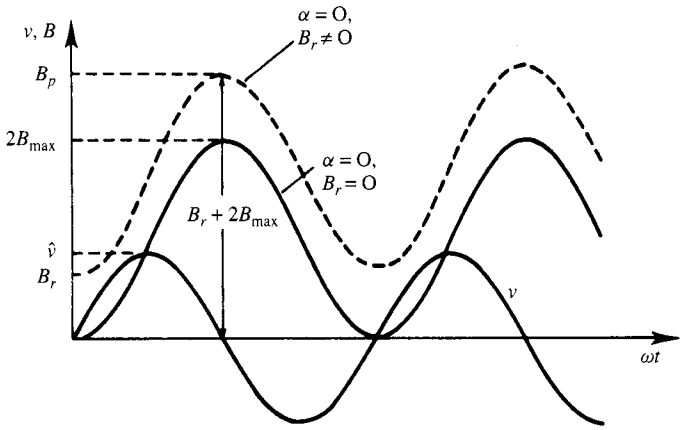

Figure 3.4 Transformer energisation flux density with and without remanence

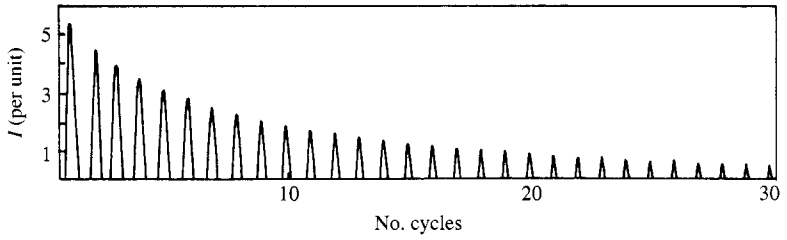

Figure 3.5 Inrush current of a 5 MVA transformer: $B_r = 1.3$ T, $\alpha = 0$

$B_r + 2B_{max}$ (almost three times the working flux). For a normally designed transformer this can create peak flux densities of about 3.4 or 4.7 T, respectively [2]. When this is compared to the saturation flux density levels of around 2.05 T to be expected from symmetrical overexcitation, it can be seen that the transformer core will be driven to extreme saturation levels and will thus produce excessive ampere-turns in the core. This effect gives rise to magnetising currents of up to 5–10 per unit of the rating (as compared to the normal values of a few percentage points). Such an inrush current is shown in Figure 3.5.

The decrement of the inrush current with time is mainly a function of the primary winding resistance. For the larger transformers this inrush can go on for many seconds because of their relatively low resistance.

By way of illustration, the Fourier series of the waveshape of Figure 3.5 yields the harmonic profile shown in Figure 3.6.

The harmonic content, shown as a percentage of the rated transformer current, varies with time, and each harmonic has peaks and nulls.

3.2.5 D.C. Magnetisation

It has been shown in previous sections that a transformer excited by sinusoidal voltage produces a symmetrical excitation current that contains only odd harmonics. If a linear

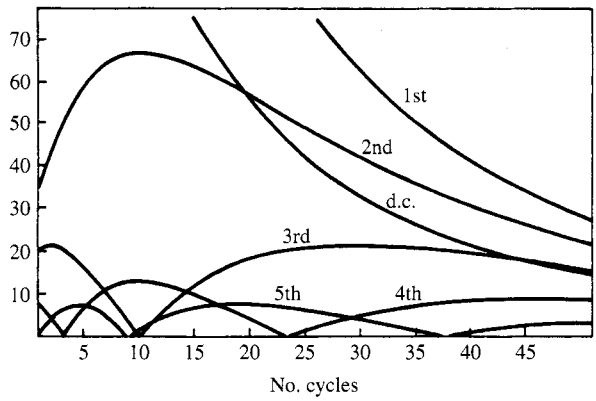

Figure 3.6 The variation of harmonic content (as a percentage of the rated current) with time

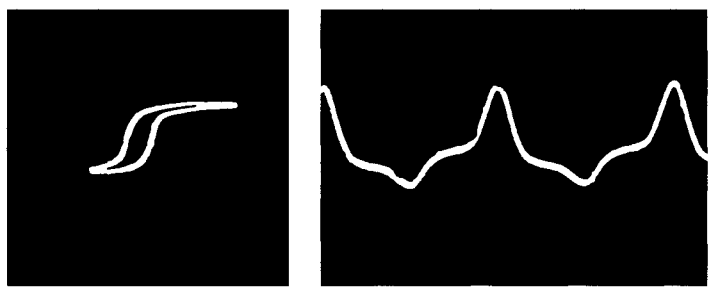

Figure 3.7 (a) Excitation characteristic; (b) exciting current waveform

or a nonlinear load is connected to this transformer, the excitation current will again contain only odd harmonics, provided that the load does not produce a direct component of current.

Under magnetic imbalance, the shape of the magnetising characteristic and the excitation current are different from those under no-load conditions. If the flux is unbalanced, as shown in Figure 3.7(a), the core contains an average value of flux ϕ_{dc} and the a.c. flux component is offset by a value equal to ϕ_{dc}. The existence of an average flux implies that a direct component of excitation current is present in Figure 3.7(b).

Under such unbalanced conditions, the transformer excitation current contains both odd and even harmonic components. The asymmetry can be caused by any load connected to the secondary of the transformer, leading to a direct component of current, in addition to the sinusoidal terms. The direct current may be a feature of the design, as in a transformer feeding a half-wave rectifier, or may result from the unbalanced operation of some particular piece of equipment, such as a three-phase converter with unbalanced firing.

A similar effect can occur as a result of geomagnetically induced currents (GIC). These are very low frequency currents (typically 0.001–0.1 Hz) and can reach levels as high as 200 A. They enter the transformer windings by way of earthed star connections and produce asymmetrical flux, causing half-cycle saturation.

It has been shown [3] that the magnitude of the harmonic components of the excitation current in the presence of direct current on the secondary side of the transformer increases almost linearly with the direct current content. The linearity is better for the lower-order harmonics.

Moreover, the harmonics generated by the transformer under d.c. magnetisation are largely independent of the a.c. excitation. Therefore there appears to be no advantage in designing a transformer to run 'underfluxed' in the presence of direct current. This independence is most noticeable at low levels of the direct current and for the lower harmonic orders.

3.3 Rotating Machine Harmonics

3.3.1 M.m.f. Distribution of A.C. Windings

Figure 3.8 shows the m.m.f. and flux distribution in one phase of a full-pitched poly-phase winding with one slot per pole per phase on the assumption of a constant air gap and in the absence of iron saturation.

Under such idealised conditions the air-gap m.m.f. is uniform and has a maximum value $(iN)/2$, where i is a maximum instantaneous current per conductor and N is the number of conductors per slot.

The frequency-domain representation of the rectangular m.m.f. space distribution of Figure 3.8 is

$$F(x) = \frac{2\sqrt{2}IN}{\pi}\left\{\sin\frac{2\pi x}{\lambda} + \frac{1}{3}\sin\left(3\frac{2\pi x}{\lambda}\right) + \frac{1}{5}\sin\left(5\frac{2\pi x}{\lambda}\right) + \cdots\right\} \tag{3.3}$$

Thus, the rectangular m.m.f. distribution is reduced to a fundamental and harmonic components. The amplitude of the nth harmonic is $1/n$ times the fundamental pole pitch.

In general, for an alternating current of angular frequency $\omega = 2\pi f$, equation (3.3) becomes

$$F(x) = \frac{2\sqrt{2}IN}{\pi}\sin(\omega t)\sum_{n=1}^{\infty}\frac{1}{n}\sin\left(n\frac{2\pi x}{\lambda}\right), \quad \text{for } n \text{ odd} \tag{3.4}$$

where λ is the wavelength and I the r.m.s. value of the current.

However, in practice the windings are distributed along the surface with g slots per pole per phase and the m.m.f.s of the g coils are displaced from each other in space.

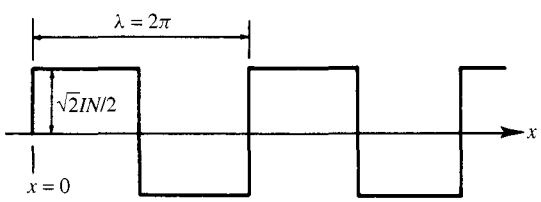

Figure 3.8 M.m.f. and flux distribution of full-pitch winding with one slot per pole

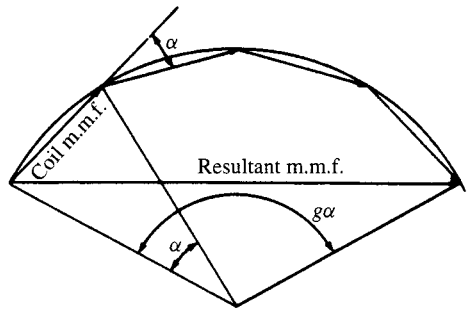

Figure 3.9 Determination of distribution factor

Moreover, the displacement angle is different for the various harmonics since their pole pitches are different.

For an m-phase machine, the number of slots per pole is $Q = mg$ and the electrical angle between slots $\alpha = \pi/Q$.

The distribution factor is

$$K_d = \frac{\text{Resultant m.m.f.}}{\text{Sum of m.m.f.s of individual coils}}.$$

From the geometry of Figure 3.9,

$$k_d = \frac{\sin(g\alpha/2)}{g\sin(\alpha/2)} \tag{3.5}$$

for the fundamental frequency, and

$$k_{dn} = \frac{\sin(ng\alpha/2)}{g\sin(n\alpha/2)} \tag{3.6}$$

for the nth harmonic.

Hence the m.m.f. of one phase of a poly-phase winding is

$$F(x) = \frac{2\sqrt{2}IN}{\pi} g\sin(\omega t)\sum_{n=1}^{\infty}\frac{k_{dn}}{n}\sin\left(n\frac{2\pi x}{\lambda}\right), \quad \text{for } n \text{ odd} \tag{3.7}$$

3.3.2 Three-Phase Winding

The phase windings of a three-phase machine are displaced by $2\pi/3$ in space and the currents by $2\pi/3$ in time. The corresponding m.m.f.s are

$$F_1(x) = \frac{2\sqrt{2}IN}{\pi} g\sin\omega t\left\{\sum_{n=1}^{\infty}\frac{k_{dn}}{n}\sin\left(n\frac{2\pi x}{\lambda}\right)\right\} \tag{3.8}$$

$$F_2(x) = \frac{2\sqrt{2}IN}{\pi} g \sin\left(\omega t - \frac{2\pi}{3}\right) \left\{\sum_{n=1}^{\infty} \frac{k_{dn}}{n} \sin\left[n\left(\frac{2\pi x}{\lambda} - \frac{2\pi}{3}\right)\right]\right\} \quad (3.9)$$

$$F_3(x) = \frac{2\sqrt{2}IN}{\pi} g \sin\left(\omega t - \frac{4\pi}{3}\right) \left\{\sum_{n=1}^{\infty} \frac{k_{dn}}{n} \sin\left[n\left(\frac{2\pi x}{\lambda} - \frac{4\pi}{3}\right)\right]\right\} \quad (3.10)$$

The total m.m.f. is $F(x) = F_1(x) + F_2(x) + F_3(x)$, and its nth harmonic term is

$$\begin{aligned}
&\frac{2\sqrt{2}IN}{\pi} g \frac{k_{dn}}{n} \left\{\sin\left(n\frac{2\pi x}{\lambda}\right) \sin\omega t + \sin\left[n\left(\frac{2\pi x}{\lambda} - \frac{2\pi}{3}\right)\right] \sin\left(\omega t - \frac{2\pi}{3}\right)\right. \\
&\quad \left. + \sin\left[n\left(\frac{2\pi x}{\lambda} - \frac{4\pi}{3}\right)\right] \sin\left(\omega t - \frac{4\pi}{3}\right)\right\} \\
&= \frac{2\sqrt{2}IN}{\pi} g \frac{k_{dn}}{2n} \left\{\cos\left[\frac{2\pi nx}{\lambda} - \omega t\right] - \cos\left[\frac{2\pi nx}{\lambda} + \omega t\right]\right. \\
&\quad + \cos\left[\frac{2\pi nx}{\lambda} - \omega t - (n-1)\frac{2\pi}{3}\right] - \cos\left[\frac{2\pi nx}{\lambda} + \omega t - (n+1)\frac{2\pi}{3}\right] \\
&\quad \left. + \cos\left[\frac{2\pi nx}{\lambda} - \omega t - (n-1)\frac{4\pi}{3}\right] - \cos\left[\frac{2\pi nx}{\lambda} + \omega t - (n+1)\frac{4\pi}{3}\right]\right\} \quad (3.11)
\end{aligned}$$

Putting in turn $n = 1, 3, 5$, etc.

$$\begin{aligned}
F(x) = \frac{3\sqrt{2}IN}{\pi} g &\left\{(k_{d1}) \cos\left(\frac{2\pi x}{\lambda} - \omega t\right) + \left(\frac{k_{d5}}{5}\right) \cos\left(5 \times \frac{2\pi x}{\lambda} + \omega t\right)\right. \\
&\left. + \left(\frac{k_{d7}}{7}\right) \cos\left(7 \times \frac{2\pi x}{\lambda} - \omega t\right) + \cdots\right\} \quad (3.12)
\end{aligned}$$

It can be seen that the fundamental is a travelling wave moving in the positive direction, triplen harmonics (3, 9, 15, etc.) are absent, the fifth harmonic is a wave travelling in the negative direction, the seventh travels in the positive direction, etc.

3.3.3 Slot Harmonics

If the machine has mg slots per pole (as shown in Figure 3.10), the variation of permeance in the air gap can be approximated by

$$A_1 + A_2 \sin\left(2mg\frac{2\pi x}{\lambda}\right) \quad (3.13)$$

Since the fundamental m.m.f. varies as $B\sin(2\pi x/\lambda)$, the resultant flux density variation is

$$\left\{B \sin\frac{2\pi x}{\lambda}\right\} \left\{A_1 + A_2 \sin\left(2mg\frac{2\pi x}{\lambda}\right)\right\} \quad (3.14)$$

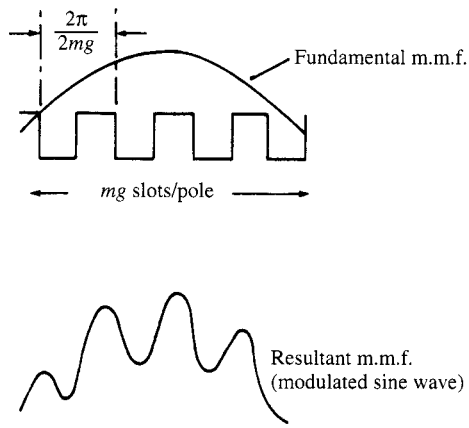

Figure 3.10 Slot harmonics

which has a fundamental frequency component, i.e.

$$A_1 B \sin\left(\frac{2\pi x}{\lambda}\right) \tag{3.15}$$

and frequency components expressed as

$$A_2 B \sin\frac{2\pi x}{\lambda} \sin\left(2mg\frac{2\pi x}{\lambda}\right) = \frac{A_2 B}{2}\left\{\cos\left(\frac{2\pi x}{\lambda}(2mg-1)\right) - \cos\left(\frac{2\pi x}{\lambda}(2mg+1)\right)\right\} \tag{3.16}$$

Therefore slotting gives rise to harmonics of orders $2mg \pm 1$.

3.3.4 Voltage Harmonics Produced by Synchronous Machines

If the magnetic flux of the field system is distributed perfectly sinusoidally around the air gap, then the e.m.f. generated in each full-pitched armature coil is $2\pi f\phi \sin \omega t$ volts per turn. Here ϕ is the total flux per pole and the frequency f is related to speed N (in revolutions per second) and pole pairs p by $f = Np$. However the flux is never exactly distributed in this way, particularly in salient pole machines. A non-sinusoidal field distribution can be expressed as a harmonic series:

$$F(x) = F_1 \sin\left(\frac{2\pi x}{\lambda}\right) + F_3 \sin\left(\frac{3 \times 2\pi x}{\lambda}\right) + F_5 \sin\left(\frac{5 \times 2\pi x}{\lambda}\right) + \cdots \tag{3.17}$$

The machine can be considered to have $2p$ fundamental poles together with $6p$, $10p$, ..., $2np$ harmonic poles, all individually sinusoidal and all generating e.m.f.s in an associate winding. The winding e.m.f. can be expressed as a harmonic series:

$$E(t) = E_1 \sin \omega t + E_3 \sin 3\omega t + E_5 \sin 5\omega t + \cdots \tag{3.18}$$

The magnitudes of the harmonic e.m.f.s are determined by the harmonic fluxes, the effective electrical phase spread of the winding, the coil span, and the method of interphase connection.

For an integral slot winding with g slots per pole per phase and an electrical angle α between slots, the distribution factor for the nth harmonic is

$$k_{dn} = \frac{\sin(ng\alpha/2)}{g\sin(n\alpha/2)} \tag{3.19}$$

If the coils are chorded to cover $(\pi \pm \theta)$ electrical radians, the flux linked is reduced by $\cos(\theta/2)$ and the e.m.f. is reduced in proportion. The effective chording angle for harmonics of order n is $n\theta$. Hence the general coil-span factor is

$$k_{sn} = \cos(n\theta/2) \tag{3.20}$$

By suitable choice of k_d and k_s many troublesome e.m.f. harmonics can be minimised or even eliminated. The triplen harmonics in a three-phase machine are generally eliminated by phase connection, and it is usual to select the coil span to reduce fifth and seventh harmonics.

Standby generators with neutral require special consideration in this respect, as illustrated by the following example.

A standby generator had to be designed to supply a 250 kVA load consisting mainly of fluorescent lighting appliances. A neutral current of 40 A was considered sufficient for the generator design. However, in practice the machine generated 250 A of third-harmonic zero sequence and had to be rewound with a two-thirds pitch (i.e. $k_{s3} = \cos(3 \times 60/2) = 0$).

Slotting (the slots being on the stator) produces variation of permeance, which may be represented as $A_2 \sin[2mg(2\pi x/\lambda)]$. The fundamental rotor m.m.f. can be represented as a travelling wave $F_1 \cos[(2\pi x/\lambda - \omega t)]$. The slot ripple component of flux density is of the form

$$F_1 A_2 \sin\left(2mg\frac{2\pi x}{\lambda}\right)\cos\left(\frac{2\pi x}{\lambda} - \omega t\right) \tag{3.21}$$

This can be resolved into two counter-rotating components, i.e.

$$\frac{F_1 A_2}{2}\left\{\sin\left[(2mg+1)\frac{2\pi x}{\lambda} - \omega t\right] + \sin\left[(2mg-1)\frac{2\pi x}{\lambda} + \omega t\right]\right\} \tag{3.22}$$

which are slow-moving multi-pole harmonics. Their wavelengths are $\lambda/(2mg \pm 1)$ and the corresponding velocities are $f\lambda/(2mg \pm 1)$. As the number of waves passing any point on the stator per second is (speed $\div$ wavelength), obviously each component induces an e.m.f. of fundamental frequency in the armature.

Relative to the rotor, however, these two waves have different velocities. The rotor velocity being $f\lambda$, the waves travel at velocities $f\lambda - [f\lambda/(2mg+1)]$ and $f\lambda + [f\lambda/(2mg-1)]$ with respect to the rotor. In any closed rotor circuit each of these will generate currents of frequency $2mgf$ (by considering the ratio of speed to wavelength) and these superimpose a time-varying m.m.f. at frequency $2mgf$ on the rotor

fundamental m.m.f. This can be resolved into two counter-rotating components relative to the rotor, each travelling at high velocity $2mgf\lambda$, and therefore at $2mgf\lambda \pm f\lambda$ relative to the stator. The resultant stator e.m.f.s have frequencies $(2mg \pm 1)f$.

Slot harmonics can be minimised by skewing the stator core, displacing the centre line of damper bars in successive pole faces, offsetting the pole shoes in successive pairs of poles, shaping the pole shoes, and by the use of composite steel–bronze wedges for the slots of turboalternators.

It can be shown that the distribution factor for slot harmonics is the same as for the fundamental e.m.f.; it is not reduced by spreading the winding. Fractional instead of integral slotting should be used.

3.3.5 Rotor Saliency Effects

In the extreme case of perfect saliency, the flux concentrates exclusively in the direct axis of the rotor. If the stator current is of positive sequence, the field produced by this current in the rotor is stationary, and only causes armature reaction at the fundamental frequency. On the other hand, the flux produced by a negative sequence stator current can be divided into two components rotating in opposite senses, which therefore induce two e.m.f.s in the stator, one of them of negative sequence at the fundamental frequency and the other of positive sequence at third harmonic. The latter, using the same reasoning, will produce fifth-harmonic voltage and this in turn will create some seventh harmonic, etc. This mechanism is illustrated in Figure 3.11 for the case of a machine connected to an asymmetrical transmission line.

The above reasoning can be extended to the presence of harmonic currents in the stator. If the stator contains a current of harmonic order h and positive sequence, the rotor flux will include two opposite rotating fields of order $(h-1)$ that will induce a positive sequence voltage of order h and a negative sequence voltage of order $(h-2)$. Similarly the negative sequence current of order h will produce two opposite rotating fields of order $(h+1)$ that will cause a negative sequence voltage of order h and another positive sequence of order $(h+2)$. This effect is illustrated in Figure 3.12 with reference to the presence of seventh harmonic, of either positive or negative sequence.

In practice, as the machine poles are not completely salient and the transmission line is approximately symmetrical, the effect discussed above is not significant. Consequently, when carrying out harmonic penetration studies, the salient pole effect is normally neglected and the synchronous machine represented as a linear impedance.

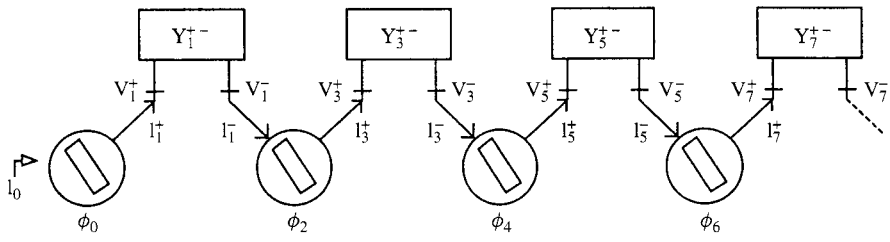

Figure 3.11 Mechanism of harmonic generation in a machine with salient poles

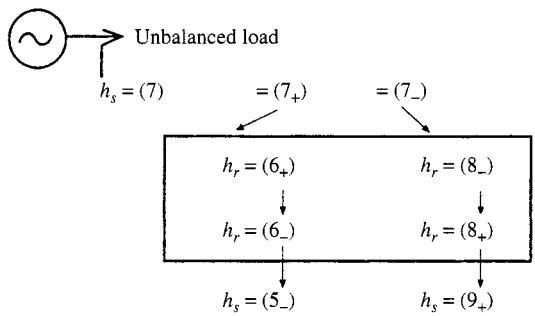

Figure 3.12 Response of a salient-pole synchronous generator to the presence of a harmonic current

However, in special cases when either the load is asymmetrical or the generator feeds static converter equipment the machine can be an important source of harmonic generation.

3.3.6 Voltage Harmonics Produced by Induction Motors

The speed of the synchronous rotating field of the stator of an induction motor is the fundamental frequency times the wavelength, i.e. $f_1\lambda$. For a slip s, the rotor speed is thus $f_1\lambda(1-s)$ and the frequency of the rotor currents sf_1.

Time harmonics are produced by induction motors as a result of the harmonic content of the m.m.f. distribution and are speed dependent.

A harmonic of order n in the rotor m.m.f. (i) has a wavelength λ/n; (ii) travels at a speed $\pm(sf)\lambda/n$ with respect to the rotor; and (iii) travels at a speed $f\lambda(1-s) \pm (sf)\lambda/n$ with respect to the stator.

This harmonic induces an e.m.f. in the stator at a frequency equal to the ratio speed ÷ wavelength, i.e.

$$f^1 = \frac{f\lambda(1-s) \pm (sf)(\lambda/n)}{\lambda/n} = f\{n - s(n \pm 1)\} \tag{3.23}$$

the positive sign being taken when the harmonic rotor m.m.f. travels in the opposite direction to the fundamental.

Harmonics can also occur as a result of electrical asymmetry. Consider an electrically unbalanced rotor winding, the stator winding being balanced such that the supply voltage produces a pure rotating field travelling at speed $f\lambda$. Slip frequency e.m.f. is induced in the rotor but, since the rotor winding is unbalanced, both positive and negative phase sequence currents will flow, giving fields in the forward and reverse directions. These travel at speed $\pm sf\lambda$ with respect to the rotor, and therefore at $f\lambda(1-s) \pm sf\lambda$ with respect to the stator. The frequencies of stator e.m.f.s induced by these fields are f and $(1-2s)f$, the latter being considered here as a harmonic frequency. Interaction of harmonic and mains frequency currents results in beats at this low frequency $2sf$ being registered on connected meters.

Table 3.1 Typical harmonic currents produced by a wound-rotor induction motor

Frequency (Hz)	Current as a percentage of fundamental	Cause
20	3.0	Pole unbalance
40	2.4	Rotor phase unbalance
50	100.0	Fundamental mutual
80	2.3	Pole unbalance
220	2.9	5th and 7th harmonic
320	3.0	mutuals
490	0.3	11th and 13th harmonic
590	0.4	mutuals

Source: [4]

An idea of the relative magnitudes of the harmonic current produced by a wound-rotor induction motor and their cause is given in Table 3.1 for a six-pole motor running at a speed of 0.9 per unit.

3.4 Distortion Caused by Arcing Devices

The voltage-current characteristics of electric arcs are highly nonlinear. Following arc ignition the voltage decreases due to the short-circuit current, the value of which is only limited by the power system impedance.

The main harmonic sources in this category are the electric arc furnace, discharge-type lighting with magnetic ballasts, and to a lesser extent arc welders.

3.4.1 Electric Arc Furnaces

The voltage-current characteristic of an arc furnace has a quasi-trapezoidal shape and its magnitude is a function of the length of the arc. The current levels, limited mainly by the furnace cables (and leads) and transformer, can reach values of over 60 kA. Those impedances have a buffering effect on the supply voltage and thus the arcing load appears as a relatively stable current harmonic source.

However, the stochastic voltage changes due to the sudden alterations of the arc length produce a spread of frequencies, predominantly in the range 0.1–30 Hz [5] about each of the harmonics present. This effect is more evident during the melting phase, caused by continuous motion of the melting scrap and the interaction of electromagnetic forces between the arcs.

During the refining part of the process the arc is better behaved, but there is still some modulation of the arc length by waves on the surface of the molten metal.

Typical time-averaged frequency spectra of the melting and refining periods are shown in Figure 3.13.

However, the levels of harmonic currents vary markedly with time, and are better displayed in the form of probabilistic plots, such as that shown in Figure 3.14.

Three sets of averaged harmonic current levels obtained by different investigators are listed in Table 3.2 as percentages of the fundamental.

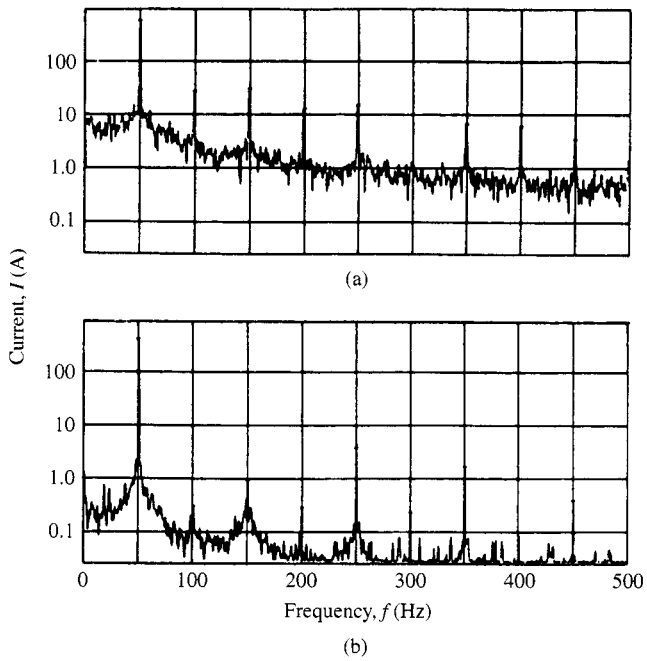

Figure 3.13 Frequency spectra for (a) melting and (b) refining periods

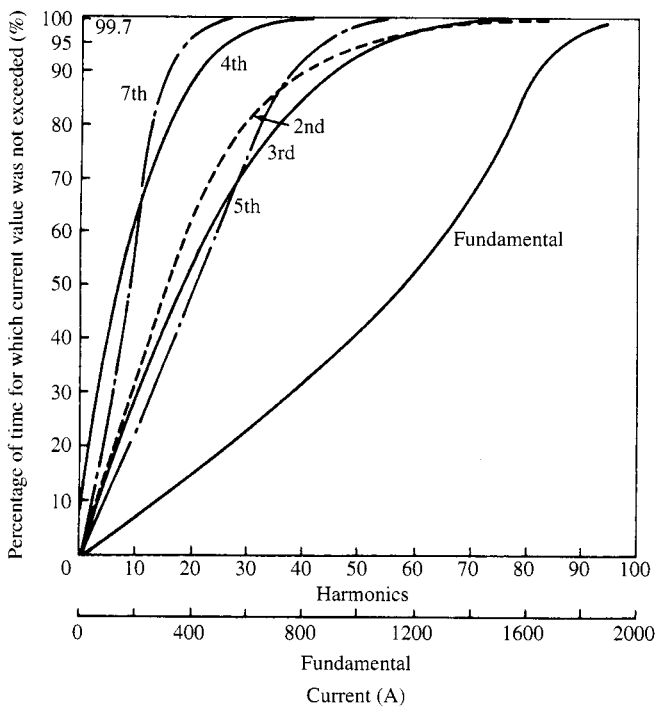

Figure 3.14 Probabilistic harmonic magnitude plots

Table 3.2 Average harmonic levels from arc furnaces expressed as percentages of the fundamental

Order	Level		
	[7]	[5]	[6]
2	3.2	4.1	4.5
3	4.0	4.5	4.7
4	1.1	1.8	2.8
5	3.2	2.1	4.5
6	0.6	Not given	1.7
7	1.3	1.0	1.6
8	0.4	1.0	1.1
9	0.5	0.6	1.0
10	>0.5	>0.5	>1.0

Note: [6] also found levels of 1% at the 22nd harmonic

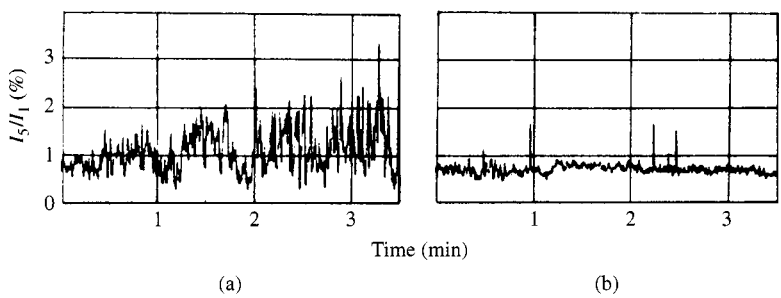

Figure 3.15 Fifth harmonic as a percentage of the fundamental with time [5]: (a) melting; (b) refining

Finally, the time variation of the harmonic currents is exemplified by the records shown in Figure 3.15 for the fifth harmonic, an important point being that the harmonic current varies not only with time but also in respect to the fundamental component.

3.4.2 Discharge-Type Lighting

Luminous discharge lighting is highly nonlinear and gives rise to considerable odd-ordered harmonic currents. This effect is clearly illustrated in Figure 3.16, which shows the current waveform and harmonic spectrum of a high-efficiency lamp.

This effect is particularly important in the case of fluorescent lamps, given the large concentration of this type of lighting. Additional magnetic ballasts are needed to limit the current to within the capability of the fluorescent tube and stabilise the arc.

In a three-phase, four-wire load the triplen harmonics are basically additive in the neutral, the third being the most dominant.

With reference to the basic fluorescent circuit of Figure 3.17, a set of voltage and current oscillograms is displayed in Figure 3.18. These waveforms are shown with

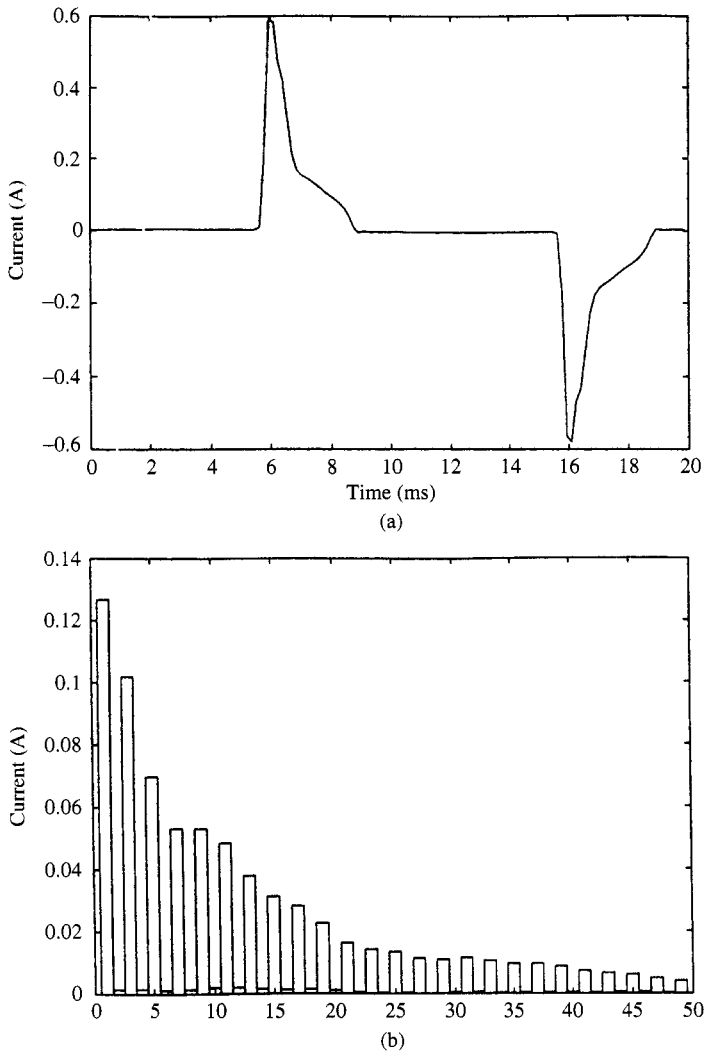

Figure 3.16 Current wave (a) and spectrum (b) of a high-efficiency discharge lamp

reference to the sinusoidal phase voltage supply. The voltage across the tube itself (Figure 3.18(a)) clearly illustrates the nonlinearity. The waveform in Figure 3.18(b) shows the phase current, and the waveform in Figure 3.18(c) the neutral current for a case of three banks of three lamps connected in star. The latter consists almost exclusively of third harmonic.

Lighting circuits often involve long distances and have very little load diversity. With individual power factor correction capacitors, the complex LC circuit can approach a condition of resonance at third harmonic. This effect has been illustrated by laboratory results in a balanced three-phase fluorescent lamp installation [8]. The results of greatest interest refer to the effects of increasing the neutral reactance and isolating the capacitor star point (see Figure 3.17). In the graph of Figure 3.19 the abscissa used is

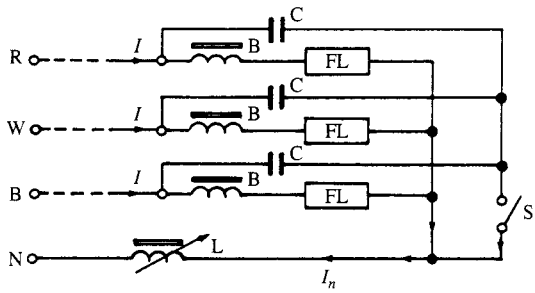

Figure 3.17 Three-phase fluorescent lighting test circuit. FL, fluorescent lamp; B, ballast; C, power factor correction capacitor; L, variable inductor; S, switch to isolate capacitor star point

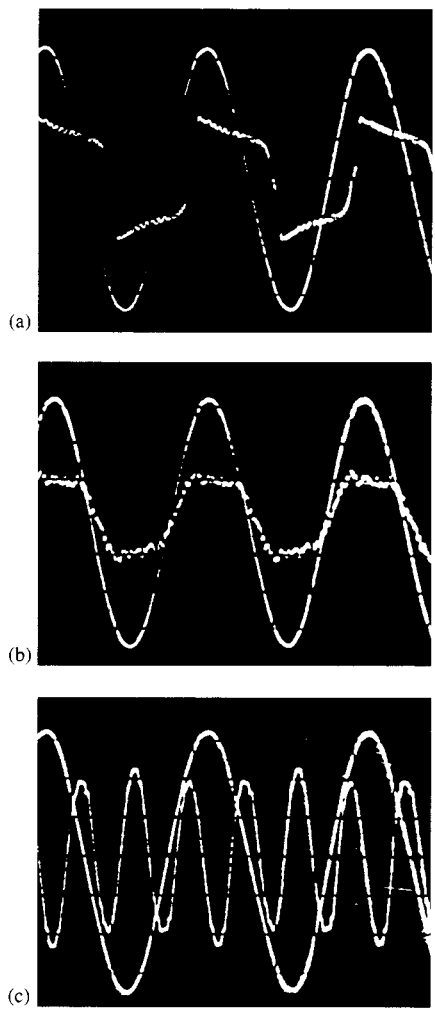

Figure 3.18 (a) Tube voltage; (b) phase current with capacitor, one lamp, 240 mA/division; (c) neutral current, three banks of three lamps in star, 240 mA/division

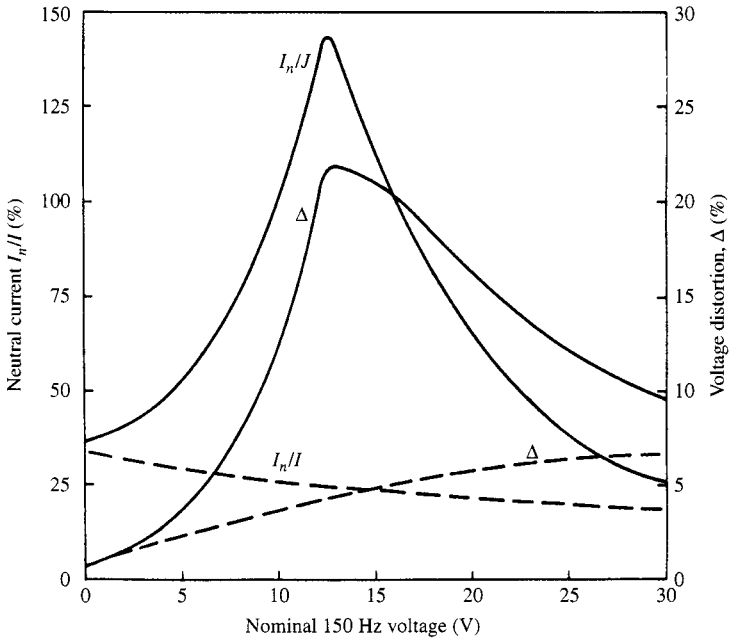

Figure 3.19 Characteristics of the fluorescent lighting test circuit. The nominal 150 Hz voltage is the calculated product of the 150 Hz lamp current per phase and the circuit zero-sequence impedance (150 Hz). (———), Switch S closed (star point connected to neutral); (- - - -), switch S open (star point floating)

the nominal third harmonic voltage, i.e. the product of the lamp third harmonic current per phase and the corresponding circuit third harmonic zero-sequence impedance. It can be seen that with the capacitor star point connected to the neutral, the third harmonic neutral current can by far exceed the nominal value calculated by the conventional method based on three times the nominal lamp current. With the star point disconnected the neutral current is less than the nominal value.

The results demonstrated in the laboratory test were in fact a confirmation of actual field test results taken on a 900 kVA fluorescent installation. In this case the full load condition operated well above the resonant point; at about half load some neutral current values exceeded the corresponding phase current values, and the voltage distortion at some distribution boards exceeded 20%.

Whenever possible, the design procedure recommended to avoid resonance is to try to avoid individual lamp compensation, providing, instead, capacitor banks adjacent to distribution boards connected either in star with floating neutral or in delta.

3.5 Single-Phase Rectification

3.5.1 D.C. Power Supplies

Many commercial and domestic appliances require direct current for their operation. The single-phase diode bridge rectifier (Figure 3.20) has become a popular power

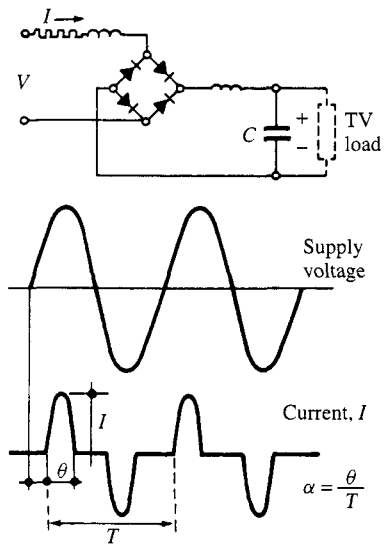

Figure 3.20 Single-phase diode rectifier bridge and d.c. capacitor power source

source for these appliances because of its reduced cost and relatively low sensitivity to supply voltage variations under normal operating conditions.

The circuit of Figure 3.20 produces a very narrow current pulse at every half-cycle of the supply frequency, because the d.c. capacitor is recharged only when the supply voltage exceeds the d.c. level (i.e. close to the peak of the voltage sine wave).

The Fourier series of the current pulse of Figure 3.20 has the expression:

$$I_n = \frac{8\alpha I}{\pi} \sum_{n=1,3,5}^{\infty} \frac{\cos n\alpha\pi}{1 - n^2\alpha^2\pi^2} \cos n\omega t \tag{3.24}$$

where I is the impulse peak value and $\alpha = \theta/T$ its duration as a proportion of the fundamental wave.

Earlier technology used a transformation stage to control the required low voltage levels and the transformer leakage inductance had a smoothing effect that resulted in low harmonic current levels.

Instead, modern appliances use the switch-mode power supply concept, whereby the input rectifier is directly connected to the a.c. source, as in Figure 3.20; however, in this case the rectified voltage is converted back to a.c. at a very high frequency and then rectified again. This process provides a very compact design and efficient operation, tolerating large variations in input voltage. Personal computers and most office and domestic appliances, as well as the electronic ballast of modern fluorescent lighting systems, are now of this type. However, the lack of a.c. side inductance smoothing lets the narrow current pulses pass directly into the a.c. system, thus increasing considerably the current harmonic content. Particularly troublesome is the third harmonic, which adds arithmetically in the neutral of the three-phase network.

The current harmonics calculated from equation (3.24) assume that the supply voltage is itself undistorted. In practice, however, the accumulation of current pulses, placed

at the centre of the voltage waveform, flattens the voltage sine wave at the peak; the flat top has the effect of widening the current pulses used to charge the capacitors, thus reducing the harmonic current injections.

Typical examples of single-phase distorting appliances are TV receivers, personal computers and microwave ovens.

TV Receivers Figure 3.21 shows the current waveform and its harmonic spectrum (as a percentage of the fundamental component) of a 23″ TV set obtained from a harmonic analyser. The main harmonics are in order of magnitude the third, fifth, seventh and ninth.

PC and Printer Figure 3.22 shows the harmonic spectrum generated by a combination of a personal computer and a printer. Again, the main component is the third (72%), followed by the fifth (60%), seventh (40%) and ninth (22.6%).

To illustrate the cumulative effect of this type of load, imagine the case of a high office block, which may have up to 1000 personal computers. If a 1000 kVA, 11 kV/440 V transformer supplies the building at say 0.95 power factor, the rated fundamental current will be 1248 A. From the spectrum of Figure 3.22, and assuming a

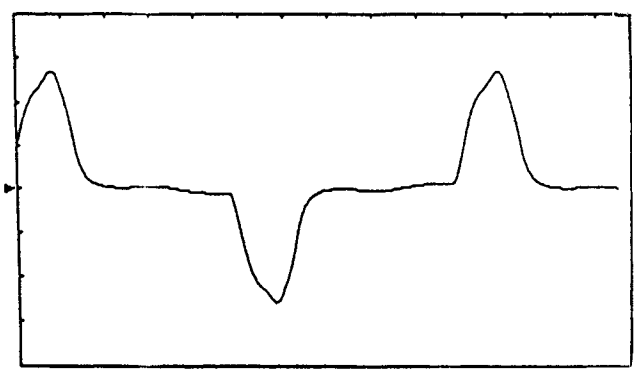

(a)

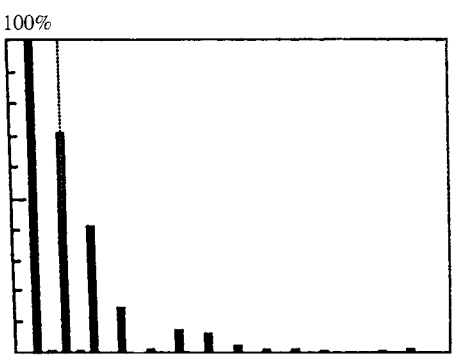

(b)

Figure 3.21 (a) Current waveform and (b) harmonic spectrum generated by a 23″ TV set

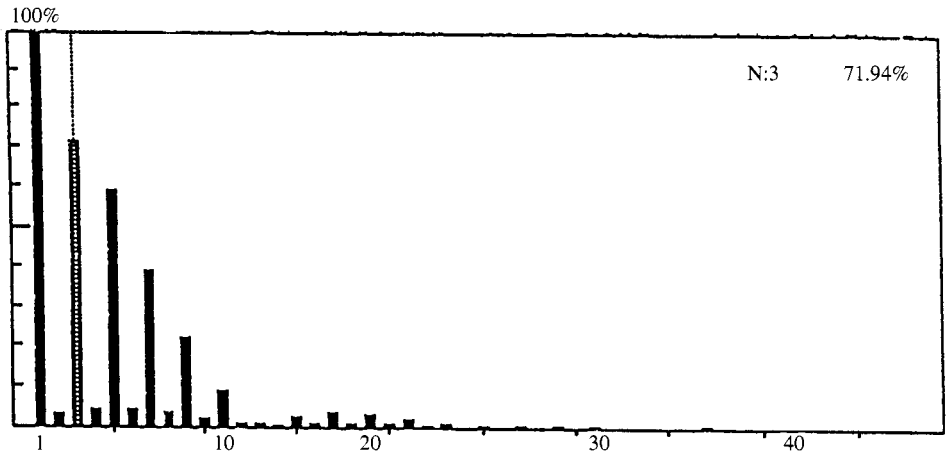

Figure 3.22 Harmonic currents generated by a PC/printer combination

1 A fundamental current per PC, the main harmonic current components per phase will be approximately:

$$I_3 = (1000/3)(0.72) = 240 \text{ A}$$
$$I_5 = (1000/3)(0.6) = 200 \text{ A}$$
$$I_7 = (1000/3)(0.4) = 133 \text{ A}$$
$$I_9 = (1000/3)(0.226) = 75 \text{ A}$$

The corresponding total demand distortion is:

$$\text{TDD}(\%) = 100\frac{\sqrt{(240^2 + 200^2 + 133^2 + 75^2)}}{1248} = 28\%$$

Moreover, the transformer neutral current will contain 720 A (3 × 240) of third harmonic and 225 A (3 × 75) of ninth harmonic, i.e. practically the same rating as the phase conductors!

Microwave Oven Figure 3.23 shows a recording of the current waveform and corresponding spectrum generated by a domestic microwave appliance, which again consists mainly of third, fifth and seventh harmonics.

3.5.2 Line-Commutated Railway Rectifiers

The application of single-phase rectification in hundreds of kilowatts is widespread in the railway electrification industry. A typical configuration of the locomotive power supply, shown in Figure 3.24, uses individual bridge control of two groups of two bridge converters connected in series to a parallel connection of two d.c. locomotive

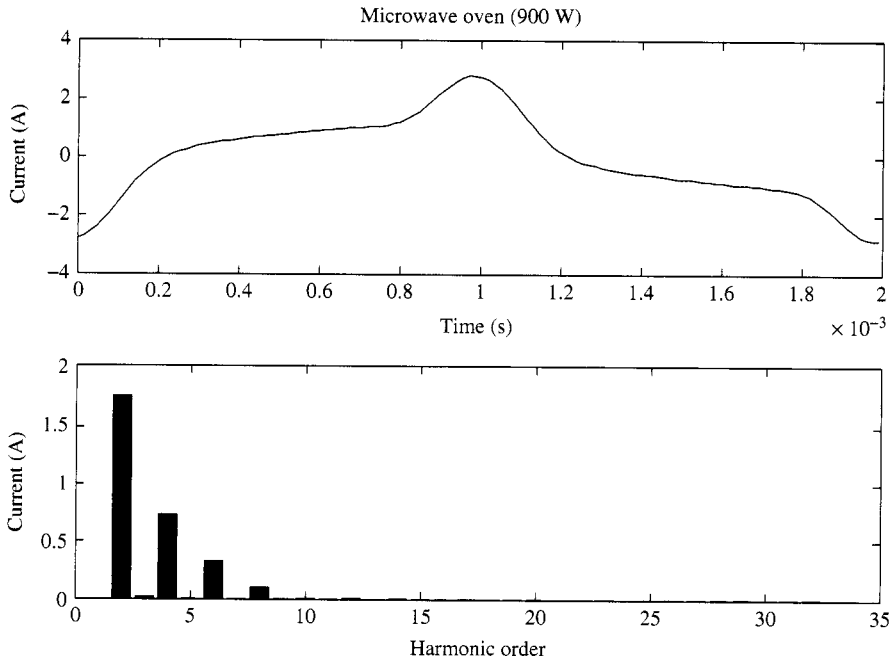

Figure 3.23 Current harmonics generated by a microwave oven

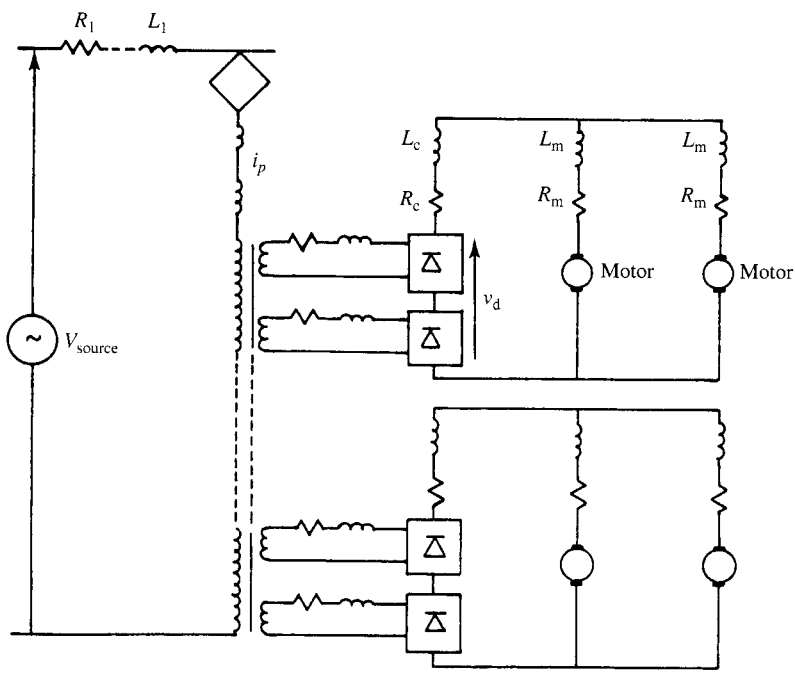

Figure 3.24 Typical locomotive power circuit

motors. At the start, the back e.m.f. of the d.c. motors is zero, the supply d.c. voltage is low and the delay angle large. Therefore during the initial accelerating period, with maximum d.c. motor current, the bridge rectifier produces the worst harmonic currents and operates with the lowest power factor. To alleviate the situation at low speeds, one of the bridges is often bypassed and phase control exercised on the other. When the speed builds up, and the second bridge operates on minimum delay, phase control is exercised on the first bridge. The relevant waveforms are illustrated in Figure 3.25.

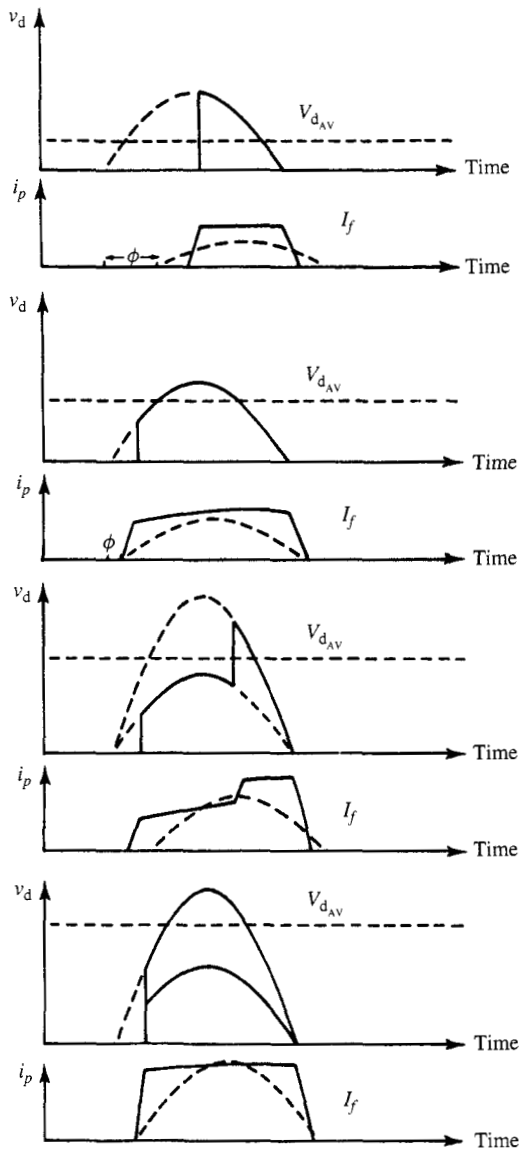

Figure 3.25 Voltage and current waveforms of a double bridge individually controlled converter

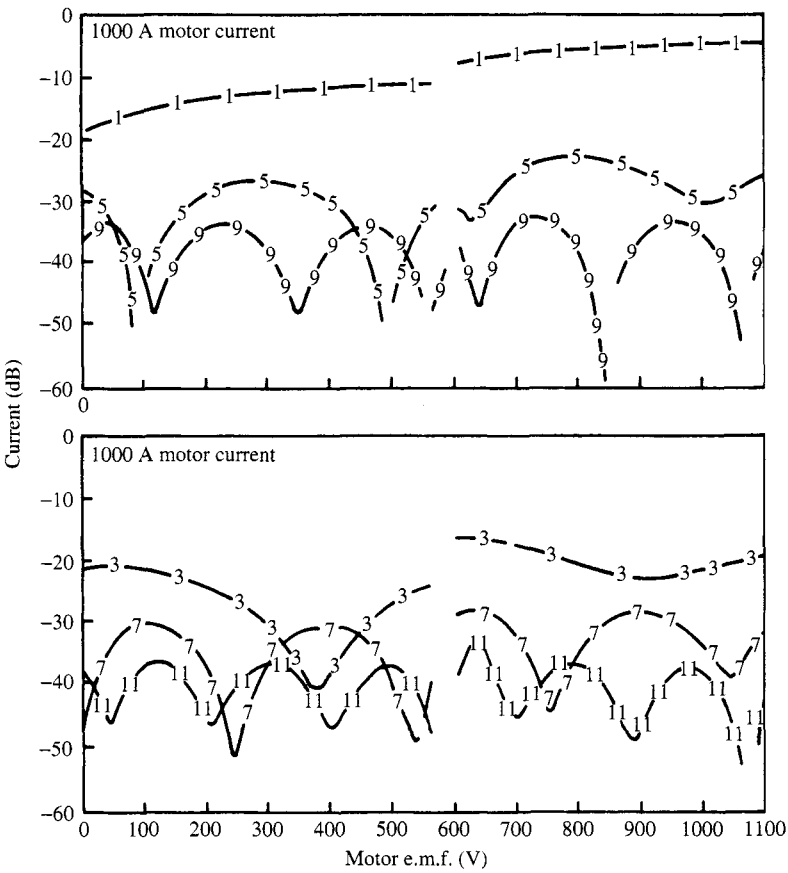

Figure 3.26 Variation in harmonic currents with locomotive operation

An indication [9] of the wide variation in harmonic current magnitudes corresponding to the waveform of Figure 3.25 is given in Figure 3.26.

3.6 Three-Phase Current-Source Conversion

A current-source converter is characterised by a very inductive d.c. side configuration relative to the a.c. system side. This is achieved by means of a series smoothing reactor on the d.c. side. As the a.c. system is predominantly inductive, some shunt capacitance (normally in the form of tuned filters) must be connected to the a.c. side of the converter. Under these conditions, the d.c. current is reasonably constant and the converter acts as a source of harmonic voltage on the d.c. side and of harmonic current on the a.c. side. The switches must block voltages of both polarities, but are only required to conduct current in one direction. Thus, large converters have traditionally been of the current-source type because of the availability of efficient highly rated thyristors.

Under perfectly symmetrical a.c. system conditions the resulting currents are exactly the same in all phases.

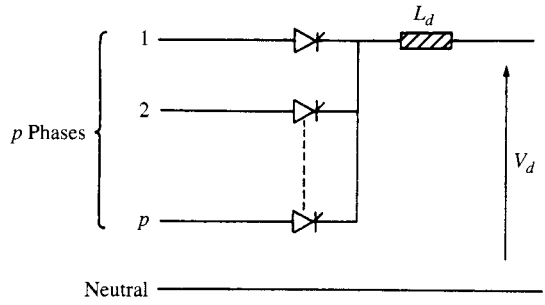

Figure 3.27 p-Phase one-way converter

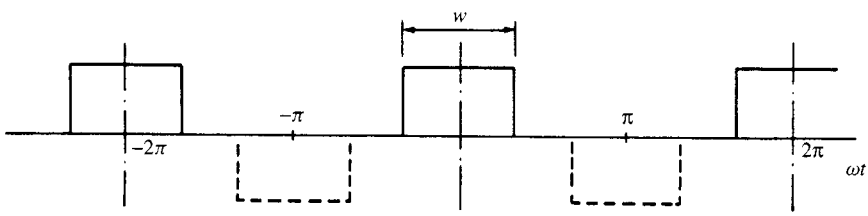

Figure 3.28 Trains of positive and negative pulses

The ideal p-phase one-way converter, illustrated in Figure 3.27, has zero a.c. system impedance and infinite smoothing inductance. Under these conditions the phase currents consists of periodic positive rectangular pulses of width $w = 2\pi/p$, repeating at the supply frequency.

If in the analysis of the waveform of Figure 3.28, the origin is taken at the centre of the pulse, $F(\omega t)$ is shown to be an 'even' function (i.e. $f(x) = f(-x)$) and the Fourier series has only cosine terms. The relevant Fourier coefficients, with reference to a 1 per unit-d.c. current, are

$$A_0 = \frac{1}{2\pi}\int_{-w/2}^{w/2} \mathrm{d}(\omega t) = \frac{w}{2\pi} = \frac{1}{p} \tag{3.25}$$

$$A_n = \frac{1}{\pi}\int_{-w/2}^{w/2} \cos(n\omega t)\,\mathrm{d}(\omega t) = \frac{2}{n\pi}\sin\left(\frac{n\pi}{p}\right) \tag{3.26}$$

The corresponding Fourier series for the positive current pulses is

$$F_p = \frac{2}{\pi}\left(\frac{w}{4} + \sin\left(\frac{w}{2}\right)\cos(\omega t) + \frac{1}{2}\sin\left(\frac{2w}{2}\right)\cos(2\omega t) + \frac{1}{3}\sin\left(\frac{3w}{2}\right)\cos(3\omega t) + \frac{1}{4}\sin\left(\frac{4w}{2}\right)\cos(4\omega t) + \cdots\right) \tag{3.27}$$

An ideal p-phase, two-way converter producing positive and negative current pulses is shown in Figure 3.29.

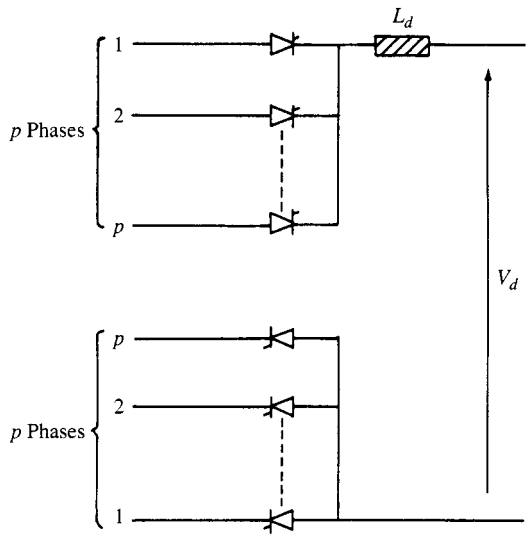

Figure 3.29 p-Phase two-way converter

Applying equations (3.25) and (3.26) to the negative group gives the following Fourier series

$$F_n = \frac{2}{\pi}\left(-\frac{w}{4} + \sin\left(\frac{w}{2}\right)\cos(\omega t) - \frac{1}{2}\sin\left(\frac{2w}{2}\right)\cos(2\omega t) + \frac{1}{3}\sin\left(\frac{3w}{2}\right)\cos(3\omega t) - \frac{1}{4}\sin\left(\frac{4w}{2}\right)\cos(4\omega t) + \cdots\right) \tag{3.28}$$

The phase current of the two-way configuration consists of alternate positive and negative pulses such that $F(\omega t + \pi) = -F(\omega t)$. Its Fourier series is obtained by combining equations (3.27) and (3.28)

$$F = F_p + F_n = \frac{4}{\pi}\left(\sin\left(\frac{w}{2}\right)\cos(\omega t) + \frac{1}{3}\sin\left(\frac{3w}{2}\right)\cos(3\omega t) + \frac{1}{5}\sin\left(\frac{5w}{2}\right)\cos(5\omega t) + \cdots\right) \tag{3.29}$$

in which the d.c. component and even-ordered harmonics have been eliminated.

For the square wave of Figure 3.30(a) $w = \pi$ which on substituting into equation (3.29) gives as the equation for the waveform in the frequency domain

$$F(t) = \frac{4}{\pi}\left(\cos(\omega t) - \frac{1}{3}\cos(3\omega t) + \frac{1}{5}\cos(5\omega t) - \frac{1}{7}\cos(7\omega t) + \cdots\right) \tag{3.30}$$

in which harmonics of order $n = 1, 5, 9$, etc. are of positive sequence and those of order $n = 3, 7, 11$, etc. are of negative sequence.

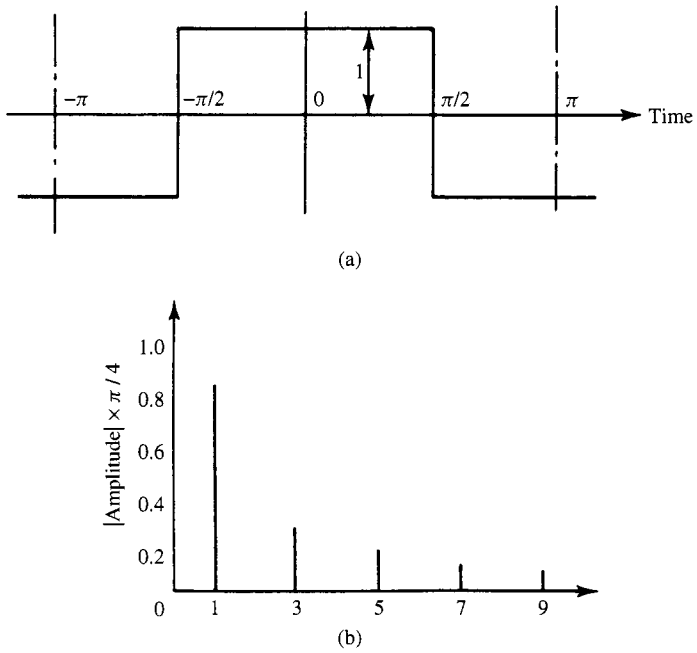

Figure 3.30 (a) Time-domain representation and (b) frequency-domain representation of a square wave

The frequency-domain representation of the square wave harmonic amplitudes is shown in Figure 3.30(b).

The time-domain waveforms can also be synthesised from the combination of the time-domain representation of the individual harmonics. Figure 3.31 shows this synthesis process for the square wave considered above. For clarity only the fundamental, third and fifth harmonics have been shown and the complex waveform produced is therefore not complete.

3.6.1 Basic (Six-Pulse) Configuration

Six-pulse rectification (and inversion) is obtained from three-phase two-way configurations. Substituting $w = 2\pi/3$ in equation (3.29) and inserting the actual d.c. current I_d, the frequency domain representation of the a.c. current in phase a is

$$i_a = \frac{2\sqrt{3}}{\pi} I_d \left(\cos(\omega t) - \frac{1}{5}\cos(5\omega t) + \frac{1}{7}\cos(7\omega t) - \frac{1}{11}\cos(11\omega t) + \frac{1}{13}\cos(13\omega t) - \frac{1}{17}\cos(17\omega t) + \frac{1}{19}\cos(19\omega t) \cdots \right) \tag{3.31}$$

The three-phase currents are shown in Figure 3.32(b), (c) and (d), respectively. Some useful observations can now be made from equation (3.31):

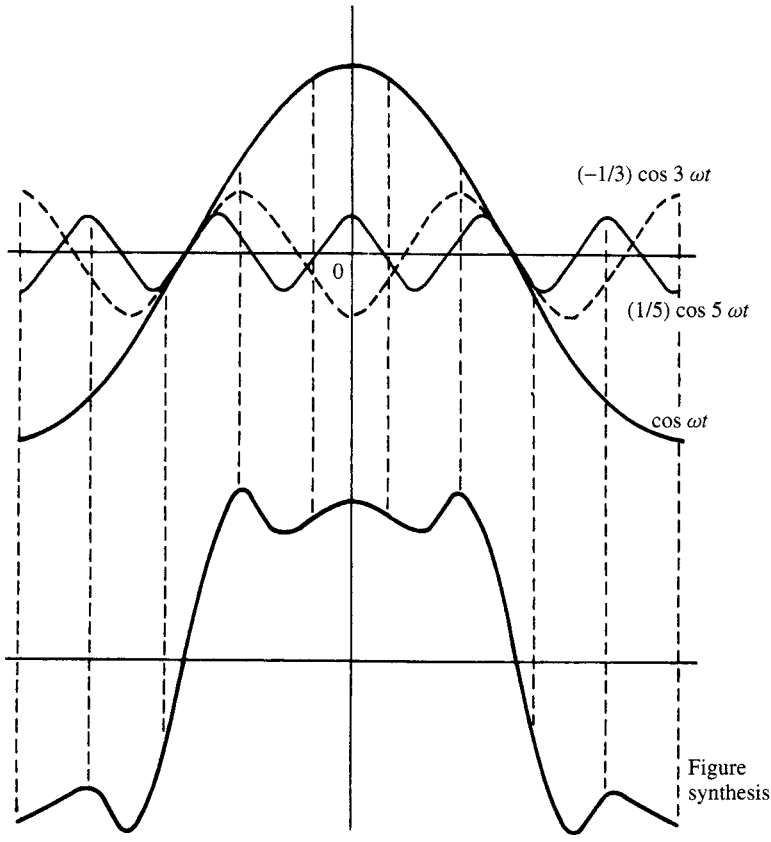

Figure 3.31 Waveform synthesis of a square wave

(1) The absence of triple harmonics.

(2) The presence of harmonics of orders $6k \pm 1$ for integer values of k.

(3) Those harmonics of orders $6k + 1$ are of positive sequence and those harmonics of orders $6k - 1$ are of negative sequence. This statement may not be obvious. Let us clarify it with reference to the fundamental, third (although not present in the symmetrical case) and fifth harmonic current components.
The three-phase currents of the fundamental frequency are

$$R(1_{\angle 0})$$
$$Y(1_{\angle -120})$$
$$B(1_{\angle 120})$$

i.e. of positive-sequence rotation.
The three-phase currents of the third harmonic component (had it existed) would be

$$R(1/3)_{\angle 0}$$

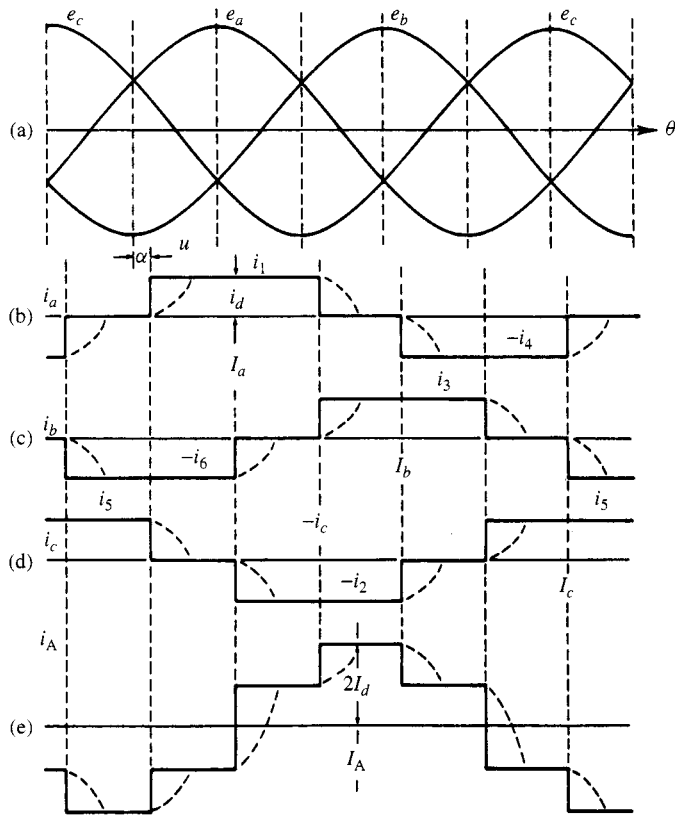

Figure 3.32 Six-pulse bridge waveforms: (a) phase to neutral voltages; (b)–(d) phase currents on the converter side; (e) phase current on the system side with delta–star transformer

$$Y(1/3)_{\angle(-120\times3)} = (1/3)_{\angle 0}$$
$$B(1/3)_{\angle(+120\times3)} = (1/3)_{\angle 0}$$

i.e. of zero-sequence rotation (however, it will be shown later that when the supply voltage is unbalanced, some positive-sequence third harmonic current will be produced).

The three-phase currents of the fifth harmonic component are

$$R(1/5)_{\angle 0}$$
$$Y(1/5)_{\angle(-120\times5)} = (1/5)_{\angle 120}$$
$$B(1/5)_{\angle(+120\times5)} = (1/5)_{\angle -120}$$

i.e. of negative-sequence rotation.

(4) The r.m.s. magnitude of the fundamental frequency is

$$I_1 = (1/\sqrt{2})(2\sqrt{3}/\pi)I_d = (\sqrt{6}/\pi)I_d \tag{3.32}$$

(5) The r.m.s. magnitude of the nth harmonic is

$$I_n = I_1/n \tag{3.33}$$

3.6.2 Effect of Transformer Connection

If either the primary or secondary three-phase windings of the converter transformer are connected in delta, the a.c. side current waveforms consist of the instantaneous differences between two rectangular secondary currents 120° apart as shown in Figure 3.32(e).

The Fourier series of the waveform shown in Figure 3.32(e) can be easily obtained from the general equation (3.29) by superimposing the results of two component pulses of widths π and $\pi/3$, respectively.

Moreover, to maintain the same primary and secondary voltages as for the star–star connection, a factor of $\sqrt{3}$ is introduced in the transformer ratio, and the current waveform is as shown in Figure 3.33.

The resulting Fourier series for the current in phase a on the primary side is

$$i_a = \frac{2\sqrt{3}}{\pi} I_d \left(\cos(\omega t) + \frac{1}{5}\cos(5\omega t) - \frac{1}{7}\cos(7\omega t) - \frac{1}{11}\cos(11\omega t) + \frac{1}{13}\cos(13\omega t) + \frac{1}{17}\cos(17\omega t) - \frac{1}{19}\cos(19\omega t) \cdots \right) \tag{3.34}$$

This series only differs from that of a star–star connected transformer by the sign of harmonic orders $6k \pm 1$ for odd values of k, i.e. the 5th, 7th, 17th, 19th, etc.

3.6.3 Twelve-Pulse Related Harmonics

Twelve-pulse configurations consist of two six-pulse groups fed from two sets of three-phase transformers in parallel, with their fundamental voltage equal and phase-shifted by 30°; a common 12-pulse configuration is shown in Figure 3.34.

Moreover, to maintain 12-pulse operation the two six-pulse groups must operate with the same control angle and therefore the fundamental frequency currents on the a.c. side of the two transformers are in phase with one another.

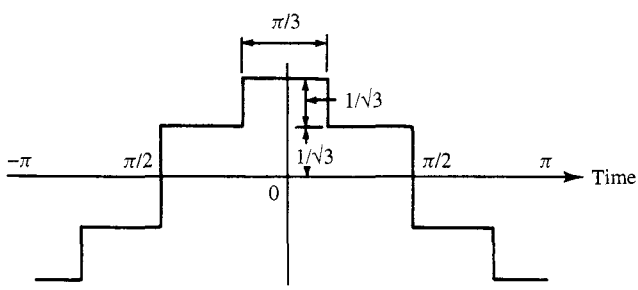

Figure 3.33 Time-domain representation of a six-pulse waveform with delta–star transformer

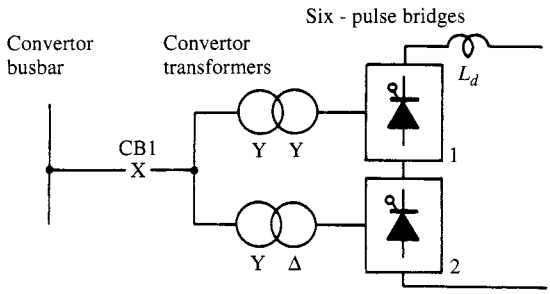

Figure 3.34 Twelve-pulse converter configuration

The resultant a.c. current is given by the sum of the two Fourier series of the star–star (equation (3.31)) and delta–star (equation (3.34)) transformers, i.e.

$$(i_a)_{12} = 2\left(\frac{2\sqrt{3}}{\pi}\right) I_d \left(\cos(\omega t) - \frac{1}{11}\cos(11\omega t) + \frac{1}{13}\cos(13\omega t) - \frac{1}{23}\cos(23\omega t) + \frac{1}{25}\cos(25\omega t)\cdots\right) \tag{3.35}$$

This series only contains harmonics of order $12k \pm 1$. The harmonic currents of orders $6k \pm 1$ (with k odd), i.e. $k = 5, 7, 17, 19$, etc., circulate between the two converter transformers but do not penetrate the a.c. network. The time-domain representation of the 12-pulse waveform is shown in Figure 3.35(a) and the corresponding frequency domain representation in Figure 3.35(b).

3.6.4 Higher-Pulse Configurations

In the last section, the use of two transformers with a 30° phase-shift has been shown to produce 12-pulse operation. The addition of further appropriately shifted transformers in parallel provides the basis for increasing pulse configurations.

For instance, 24-pulse operation is achieved by means of four transformers with 15° phase-shifts and 48-pulse operation requires eight transformers with 7.5° phase-shifts. Although theoretically possible, pulse numbers above 48 are rarely justified due to the practical levels of distortion found in the supply voltage waveforms, which can have as much influence on the voltage crossings as the theoretical phase-shifts.

Similarly to the case of the 12-pulse connection, the alternative phase-shifts involved in higher pulse configurations require the use of appropriate factors in the parallel transformer ratios to achieve common fundamental frequency voltages on their primary and secondary sides.

The theoretical harmonic currents are related to the pulse number (p) by the general expression $pk \pm 1$ and their magnitudes decrease in inverse proportion to the harmonic order. Generally harmonics above the 49th can be neglected as their amplitude is too small.

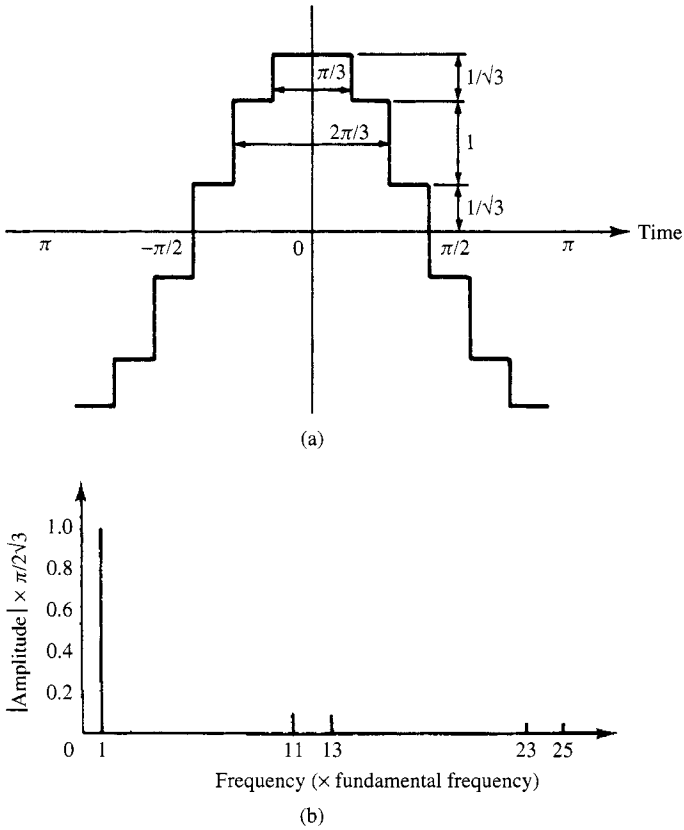

Figure 3.35 (a) Time-domain representation of the 12-pulse phase current; (b) frequency-domain representation of 12-pulse operation

3.6.5 Effect of Transformer and System Impedance

In practice the existence of reactance in the commutation circuit causes conduction overlap of the incoming and outgoing phases.

As we have seen in previous sections, high-pulse configurations are combinations of three-pulse groups, i.e. the commutation overlaps are those of the three-pulse groups as shown by the broken lines in Figure 3.32.

The current waveform has now lost the even symmetry with respect to the centre of the idealised rectangular pulse. Using as a reference the corresponding commutating voltage (i.e. the zero-voltage crossing) and assuming a purely inductive commutation circuit, the following expression defines the commutating current [10]

$$i_c = \frac{E}{\sqrt{2}X_c}(\cos(\alpha) - \cos(\omega t)) \tag{3.36}$$

where X_c is the reactance (per phase) of the commutation circuit, which is largely determined by the transformer leakage reactance.

At the end of the commutation $i_c = I_d$ and $\omega t = \mu$, and equation (3.36) becomes

$$I_d = \frac{E}{\sqrt{2}X_c}[\cos(\alpha) - \cos(\alpha + \mu)] \tag{3.37}$$

Dividing (3.36) by (3.37),

$$i_c = I_d \left(\frac{\cos(\alpha) - \cos(\omega t)}{\cos(\alpha) - \cos(\alpha + \mu)} \right) \tag{3.38}$$

and this expression applies for $\alpha < \omega t < \alpha + \mu$.

The rest of the positive current pulse is defined by

$$i = I_d \quad \text{for } \alpha + \mu < \omega t < \alpha + 2\pi/3 \tag{3.39}$$

and

$$i = I_d - I_d \left[\frac{\cos(\alpha + 2\pi/3) - \cos(\omega t)}{\cos(\alpha + 2\pi/3) - \cos(\alpha + 2\pi/3 + \mu)} \right]$$
$$\text{for } \alpha + \frac{2\pi}{3} < \omega t < \alpha + \frac{2\pi}{3} + \mu \tag{3.40}$$

The negative current pulse still possesses half-wave symmetry and therefore only odd-ordered harmonics are present. These can now be expressed in terms of the delay (firing), and overlap angles and their magnitudes, related to the fundamental components, are illustrated in Figures 3.36–3.39, for the 5th, 7th, 11th and 13th harmonics, respectively [10].

In summary, the existence of system impedance is seen to reduce the harmonic content of the current waveform, the effect being much more pronounced in the case of uncontrolled rectification. With large firing angles the current pulses are practically unaffected by a.c. system reactance.

To illustrate the use of these graphs let us consider the case of a six-pulse rectifier connected via a 50 MVA Y–Y transformer of unity turns ratio to the 110 kV system. If the rated d.c. current is 300 A, the transformer leakage reactance 10.73%, and assuming that the maximum steady-state delay is $\alpha = 30°$, determine the levels of the first four characteristic harmonic currents.

From Equation (3.37) the value of the commutation angle is:

$$\mu = \arccos\left[\cos\alpha - \frac{\sqrt{2}X_c I_d}{E} \right] - \alpha$$

where

$$X_c = x_t X_B = x_t \frac{(\text{kV})^2}{\text{MVA}} = (10.73)(110 \times 10^3)^2/(50) = 25.9\ \Omega.$$

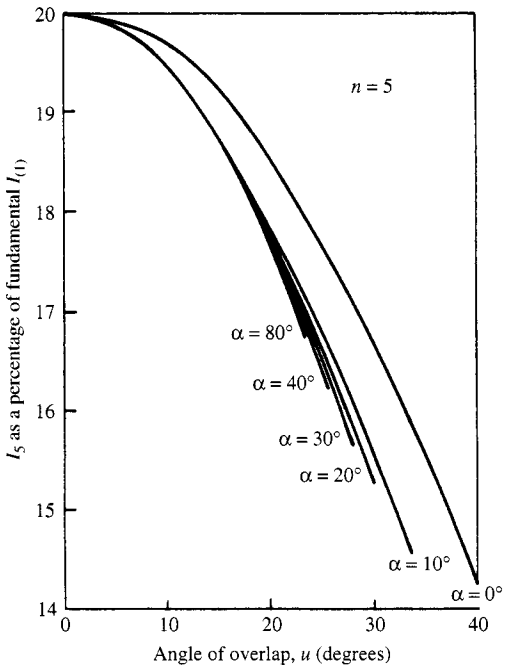

Figure 3.36 Variation of fifth harmonic current in relation to angles of delay and commutation overlap

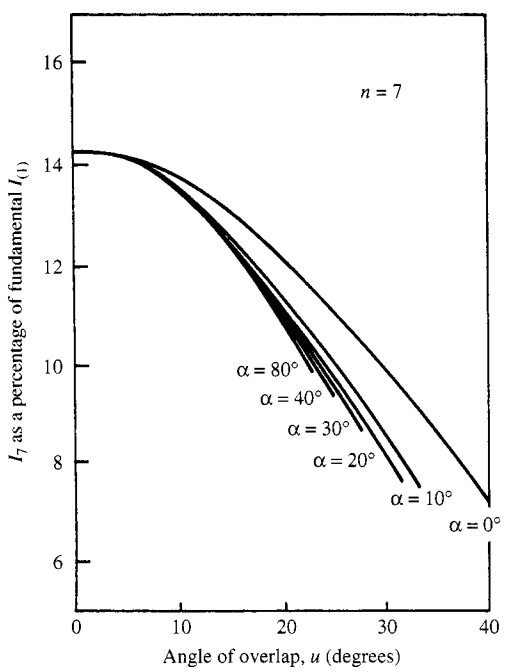

Figure 3.37 Variation of seventh harmonic current in relation to angles of delay and commutation overlap

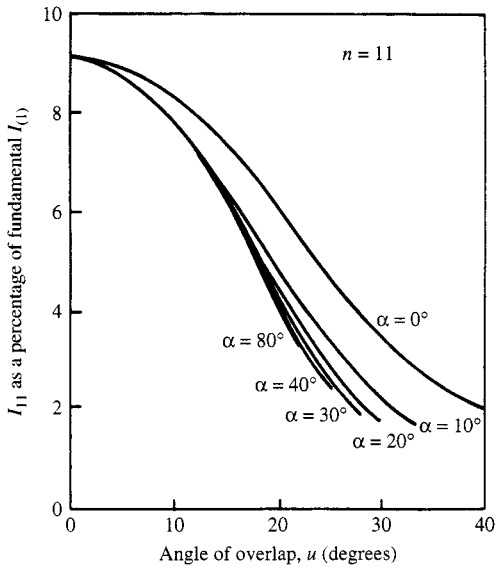

Figure 3.38 Variation of 11th harmonic current in relation to angles of delay and overlap

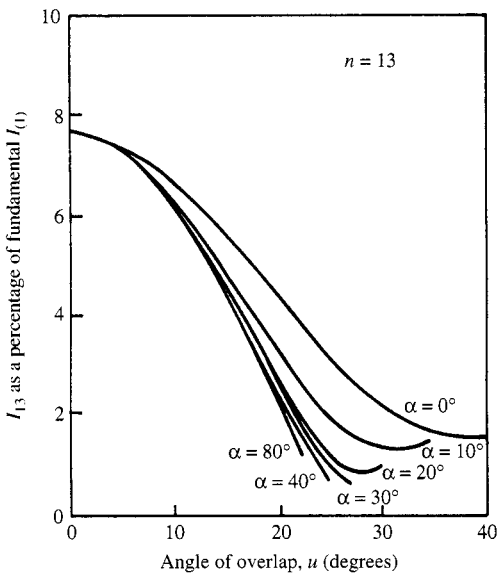

Figure 3.39 Variation of 13th harmonic current in relation to angles of delay and overlap

Therefore,

$$\mu = \arccos\left[\cos 30^\circ - \frac{\sqrt{2}(25.9)(300)}{110 \times 10^3}\right] - 30^\circ = 10^\circ$$

From Figures 3.36–3.39 the following harmonic currents as percentages of the fundamental component are obtained for $\alpha = 30°$ and $\mu = 10°$:

19.398%(5th), 13.4335%(7th), 7.772%(11th) and 6.1585%(13th)

and using equation (3.32)

$$I_1 = (\sqrt{6}/\pi)I_d = (\sqrt{6}/\pi)300 = 233.91 \text{ A}$$

Finally, the harmonic currents are:

$$I_5 = 45.37 \text{ A} \quad I_7 = 31.27 \text{ A} \quad I_{11} = 19.08 \text{ A} \quad I_{13} = 14.03 \text{ A}$$

3.6.6 Direct Voltage Harmonics

For the three-phase bridge configuration the orders of the harmonic voltages are $n = 6k$. The corresponding d.c. voltage waveforms are illustrated in Figure 3.40.

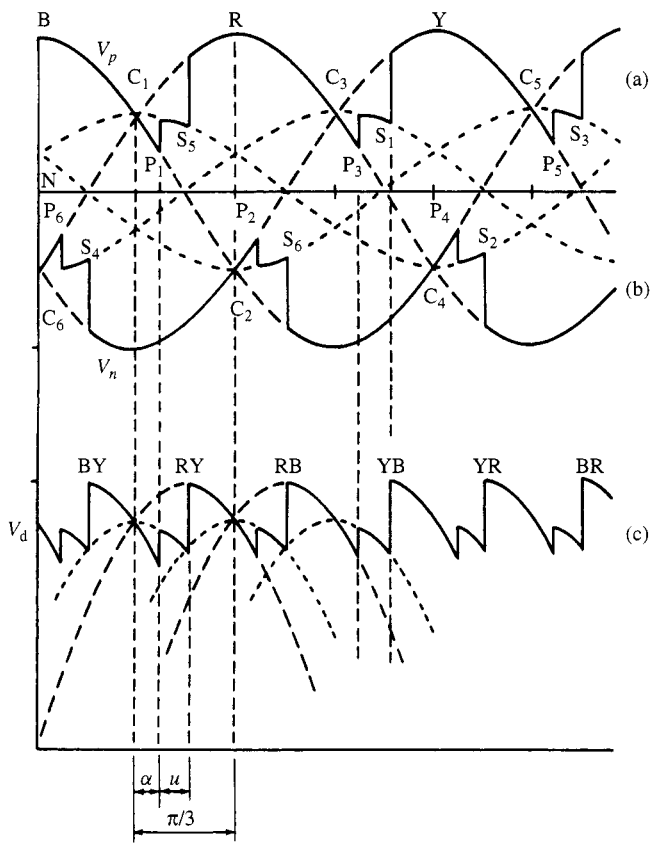

Figure 3.40 Six-pulse converter d.c. voltage waveforms: (a) at the positive terminal; (b) at the negative terminal; (c) across the output terminals

The repetition interval of the waveform shown in Figure 3.40(c) is $\pi/3$ and it contains the following three different functions with reference to voltage crossing C_1:

$$v_d = \sqrt{2}V_c \cos\left(\omega t + \frac{\pi}{6}\right) \quad \text{for } 0 < \omega t < \alpha \tag{3.41}$$

$$v_d = \sqrt{2}V_c \cos\left(\omega t + \frac{\pi}{6}\right) + \frac{1}{2}\sqrt{2}V_c \sin(\omega t) = \frac{\sqrt{6}}{2}V_c \cos(\omega t)$$
$$\text{for } \alpha < \omega t < \alpha + \mu \tag{3.42}$$

$$v_d = \sqrt{2}V_c \cos\left(\omega t - \frac{\pi}{6}\right) \quad \text{for } \alpha + \mu < \omega t < \frac{\pi}{3} \tag{3.43}$$

where V_c is the (commutating) phase to phase r.m.s. voltage.

From equations (3.41), (3.42) and (3.43) the following expression is obtained for the r.m.s. magnitudes of the harmonic voltages of the d.c. voltage waveform:

$$V_n = \frac{V_{c0}}{\sqrt{2}(n^2-1)}\left[(n-1)^2\cos^2\left((n+1)\frac{\mu}{2}\right) + (n+1)^2\cos^2\left((n-1)\frac{\mu}{2}\right)\right.$$
$$\left. - 2(n-1)(n+1)\cos\left((n+1)\frac{\mu}{2}\right)\cos\left((n-1)\frac{\mu}{2}\right)\cos(2\alpha+\mu)\right]^{\frac{1}{2}} \tag{3.44}$$

Figures 3.41 and 3.42 illustrate the variation of the 6th and 12th harmonics as a percentage of V_{c0}, the maximum average rectified voltage, which for the six-pulse bridge converter is $3\sqrt{2}V_c/\pi$. These curves and equations show some interesting facts. Firstly, for $\alpha = 0$ and $\mu = 0$, equation (3.44) reduces to

$$V_{n0} = \sqrt{2}V_{c0}/(n^2-1) \tag{3.45}$$

or

$$\frac{V_{n0}}{V_{c0}} = \sqrt{2}/(n^2-1) \approx \sqrt{2}/n^2 \tag{3.46}$$

giving 4.04%, 0.99% and 0.44% for the 6th, 12th and 18th harmonics, respectively.

Generally, as α increases, harmonics increase as well, and for $\alpha = \pi/2$ and $\mu = 0$

$$\frac{V_{n0}}{V_{c0}} = \sqrt{2}n/(n^2-1) \approx \sqrt{2}/n \tag{3.47}$$

which produces n times the harmonics content corresponding to $\alpha = 0$. This means that the higher harmonics increase faster with α. Equation (3.47) is of some importance as it represents the maximum proportion of harmonics in the system, particularly when it is considered that at $\alpha = 90°$ μ is likely to be very small.

If the converter involves two bridges, one with a star–star or delta–delta transformer and the other with a delta–star or star–delta transformer, their respective voltages will be 30° out of phase and so the harmonics will accordingly be out of phase. Since 30° of mains frequency correspond to a half-cycle of the 6th harmonic, this harmonic will be in phase opposition in the two bridges. Similarly for the 12th

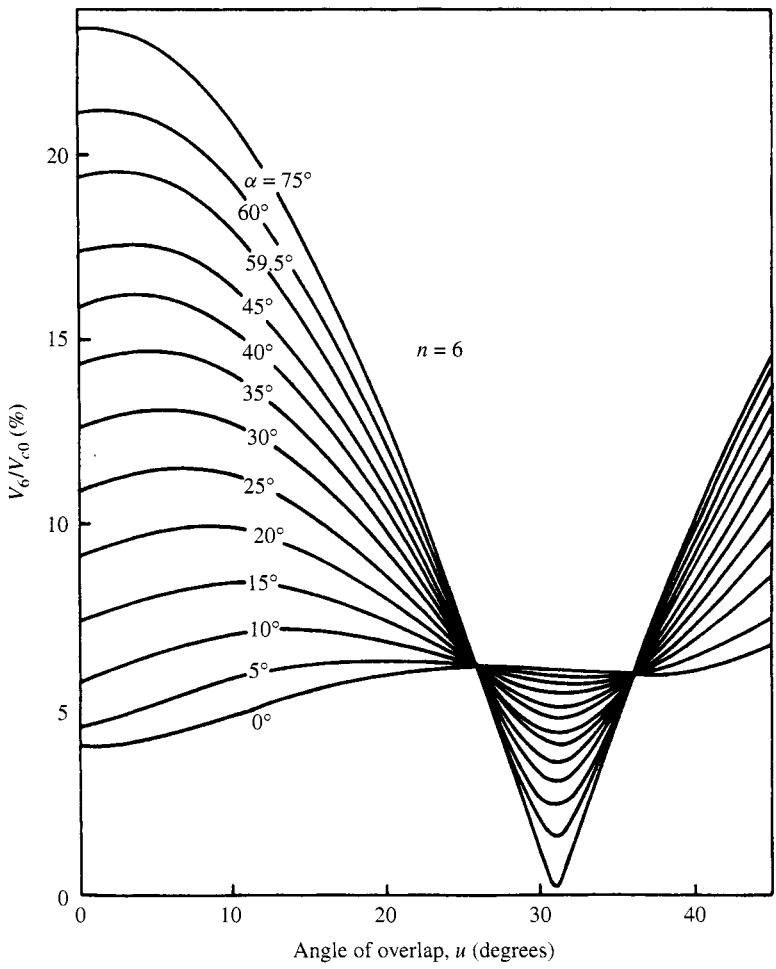

Figure 3.41 Variation of the sixth harmonic voltage in relation to angles of delay and overlap

harmonic, 30° corresponds to one cycle, giving harmonics in phase; for the 18th harmonic, 30° corresponds to one and a half cycles, giving harmonics in opposition and so on.

3.6.7 Imperfect D.C. Voltage Smoothing

Considering the limited inductance of the motor armature winding and the larger variation of firing angle, the constant d.c. current assumption of the large size converters cannot be justified in the case of a d.c. drive.

The d.c. load must now be represented as an equivalent circuit which in its simplest form includes resistance, inductance and back e.m.f. (as shown in Figure 3.43).

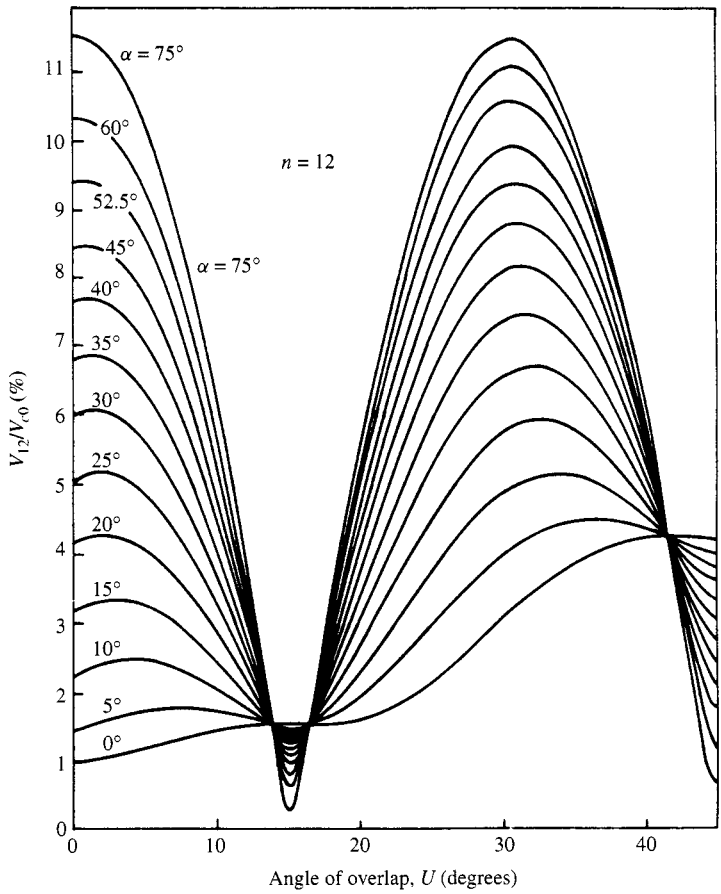

Figure 3.42 Variation of the 12th harmonic voltage in relation to angles of delay and overlap

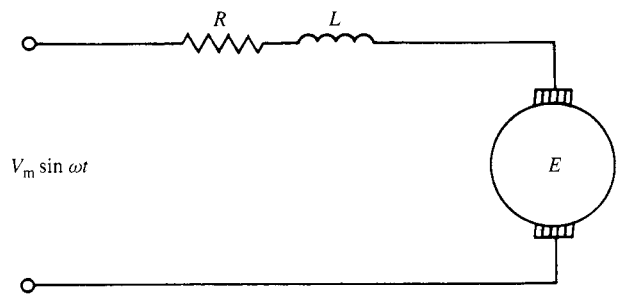

Figure 3.43 D.c. motor equivalent circuit

With sinusoidal supply voltage $V_m \sin \omega t$, the following equation applies:

$$V_m \sin(\omega t) = Ri + L\left(\frac{di}{dt}\right) + E \tag{3.48}$$

and the load current has the form

$$i = Ke^{-Rt/L} + \frac{V_m}{\sqrt{R^2 + (\omega L)^2}} \sin(\omega t - \phi) - \frac{E}{R} \tag{3.49}$$

where

$$\phi = \tan^{-1}(\omega L/R)$$

and the constant K is derived from the particular initial conditions.

Under nominal loading the firing delay is kept low, but during motor start or light load conditions the delay increases substantially and the current may even be discontinuous. This extreme operating condition is illustrated in Figure 3.44 for a six-pulse rectifier. Each phase consists of two positive and two negative current pulses, which are derived from the general expression (3.49) by using the appropriate voltage phase relationships with a common reference.

The current in phase R with reference to the instant when V_{RY} is maximum in Figure 3.44 has the following components:

(1) Over the range $\theta_1 < \omega t < \theta_2$

$$i = \frac{V_m}{R}\left(\cos(\phi)\cos(\omega t - \phi) - \frac{E}{V_m} + \left[\frac{E}{V_m} - \cos(\phi)\cos(\theta_1 - \phi)\right] e^{(-R/\omega L)(\omega t - \theta_1)}\right) \tag{3.50}$$

(2) When $\theta_3 < \omega t < \theta_4$ where $\theta_3 = (\theta_1 + \pi/3)$,

$$i = \frac{V_m}{R}\left(\cos(\phi)\cos\left(\omega t - \frac{\pi}{3} - \phi\right) - \frac{E}{V_m} + \left[\frac{E}{V_m} - \cos(\phi)\cos(\theta_1 - \phi)\right] e^{(-R/\omega L)(\omega t - \pi/3 - \theta_1)}\right) \tag{3.51}$$

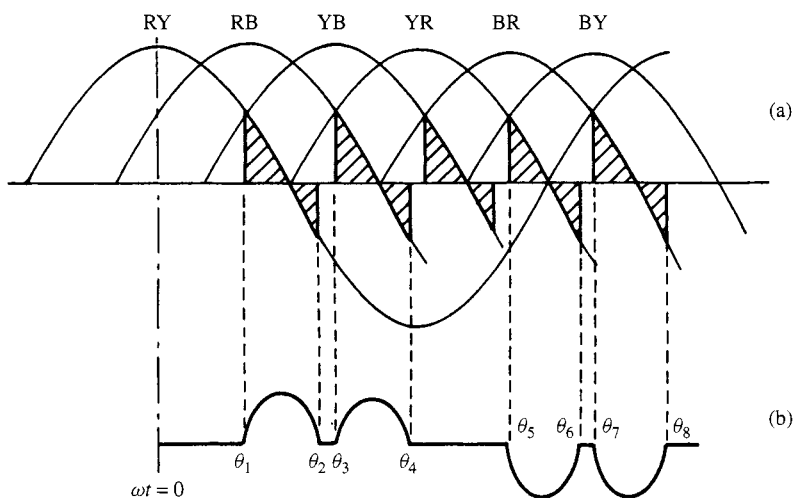

Figure 3.44 Discontinuous waveforms: (a) d.c. voltage; (b) a.c. current in phase R

(3) When $\theta_5 < \omega t < \theta_6$ where $\theta_5 = (\theta_1 + \pi)$,

$$i = -\frac{V_m}{R}\left(\cos(\phi)\cos(\omega t - \pi - \phi) - \frac{E}{V_m} + \left[\frac{E}{V_m} - \cos(\phi)\cos(\theta_1 - \phi)\right] e^{(-R/\omega L)(\omega t - \pi - \theta_1)}\right) \tag{3.52}$$

(4) When $\theta_7 < \omega t < \theta_8$ where $\theta_7 = (\theta_1 + 2\pi/3)$,

$$i = -\frac{V_m}{R}\left(\cos(\phi)\cos\left(\omega t - \frac{2\pi}{3} - \phi\right) - \frac{E}{V_m} + \left[\frac{E}{V_m} - \cos(\phi)\cos(\theta_1 - \phi)\right] e^{(-R/\omega L)(\omega t - 2\pi/3 - \theta_1)}\right) \tag{3.53}$$

Application of Fourier analysis to these current pulses indicates that the fifth harmonic can reach peak levels of up to three times those of the rectangular wave shape with the same fundamental component.

When d.c. motors are designed specifically for use with thyristor converters their armature inductance is often increased to avoid current discontinuities and the above analysis can then be simplified considerably. An approximate method described by Dobinson [11] derives the harmonic components of the a.c. current in terms of the ripple ratio, i.e.

$$r = \frac{I_r}{I_d} \tag{3.54}$$

where I_r is the alternating ripple of the direct current and I_d is the mean direct current, flowing in the motor armature circuit (Figure 3.45) at the relevant speed and load. The method ignores the effect of the commutation reactance, which at large delay angles is negligible.

With reference to Figure 3.45, a further approximation is made by assuming that the ripple is part of a sine wave displaced by a value θ relative to the zero direct-current level.

The information included in Figures 3.45(b) and (c) results in the following functions:

$$f(\theta) = 0 \qquad \text{for } 0 < \theta < \pi/6 \tag{3.55}$$

$$f(\theta) = I_d\left[7.46r\sin\left(\theta + \frac{\pi}{6}\right) - 7.13r + 1\right] \qquad \text{for } \pi/6 < \theta < \pi/2 \tag{3.56}$$

$$f(\theta) = I_d\left[7.46r\sin\left(\theta - \frac{\pi}{6}\right) - 7.13r + 1\right] \qquad \text{for } \pi/2 < \theta < 5\pi/6 \tag{3.57}$$

$$f(\theta) = 0 \qquad \text{for } 5\pi/6 < \theta < \pi \tag{3.58}$$

Application of Fourier analysis yields the following expression for the fundamental:

$$I_1 = I_d(1.102 + 0.014r) \tag{3.59}$$

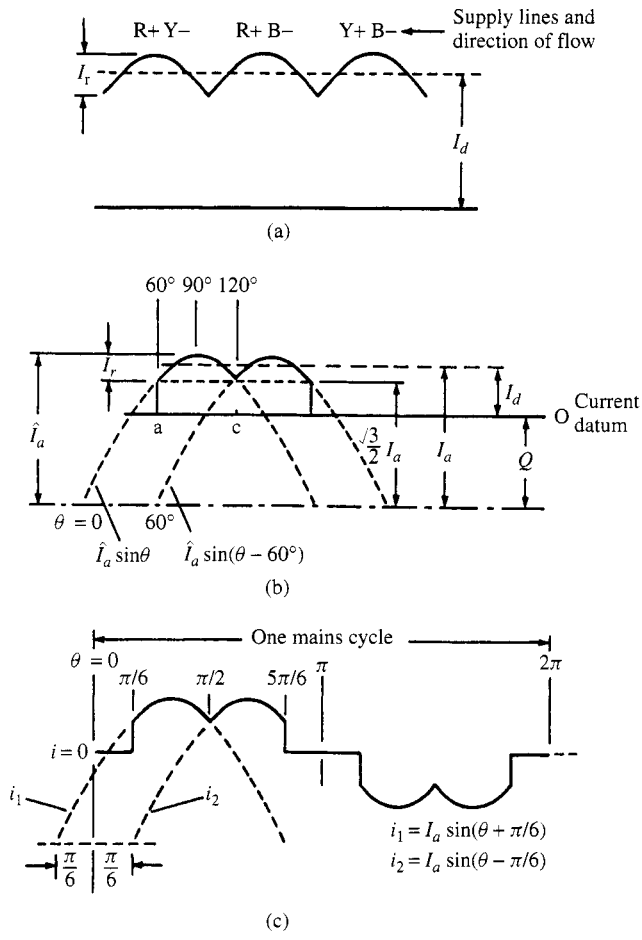

Figure 3.45 Converter output and input current waveforms: (a) armature current; (b) thyristor current; a.c. current

Also, the magnitudes of the characteristic harmonics (expressed as a percentage of the fundamental) are

$$I_n = 100\left(\frac{1}{n} + \frac{6.46r}{n-1} - \frac{7.13r}{n}\right)(-1)^k \quad \text{for } n = kp - 1 \tag{3.60}$$

and

$$I_n = 100\left(\frac{1}{n} + \frac{6.46r}{n+1} - \frac{7.13r}{n}\right)(-1)^k \quad \text{for } n = kp + 1 \tag{3.61}$$

These are plotted in Figure 3.46 as a function of r covering the whole range from zero ripple (i.e. infinite inductance) to the limit case of continuous current (at $r = 1.5$).

Figure 3.46 shows that although the fifth harmonic increases substantially with output current ripple, all the other harmonics reduce.

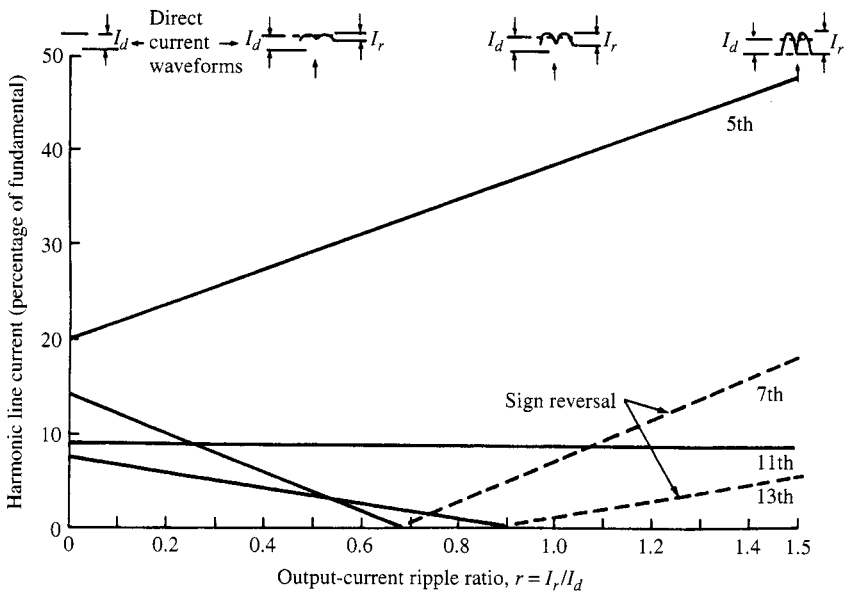

Figure 3.46 Harmonic content of the supply current for six-pulse converter with finite inductive load

3.6.8 Half-Controlled Rectification

Because of the cheapness of its design, the half-controlled version of the variable speed d.c. drive has been popular in some countries. When operating at full load (i.e. with zero firing delay) these controllers produce virtually the same harmonic currents as the fully controlled converter and operate very efficiently.

However, under operating conditions requiring firing delays, the half-wave symmetry of the current waveform is lost, as shown in Figure 3.47.

At low loads these controllers not only have a very poor power factor but introduce severe waveform distortion, particularly at even harmonics. More often than not the controllers and motors initially installed are larger than required to cope with future expansion, and operation is then at a fraction of the full load. Under these conditions the second harmonic component often reaches levels close to the fundamental current.

3.6.9 Uncharacteristic Harmonic and Inter-Harmonic Generation

The harmonic effects caused by imperfect system conditions encountered in practice cannot be derived from the idealised models described in Section 3.6.

In general each of the main three parts of the system is always in error to a lesser or greater extent:

(1) The a.c. system voltages are never perfectly balanced and undistorted, and the system impedances, in particular the converter transformer, are not exactly equal in the three phases.

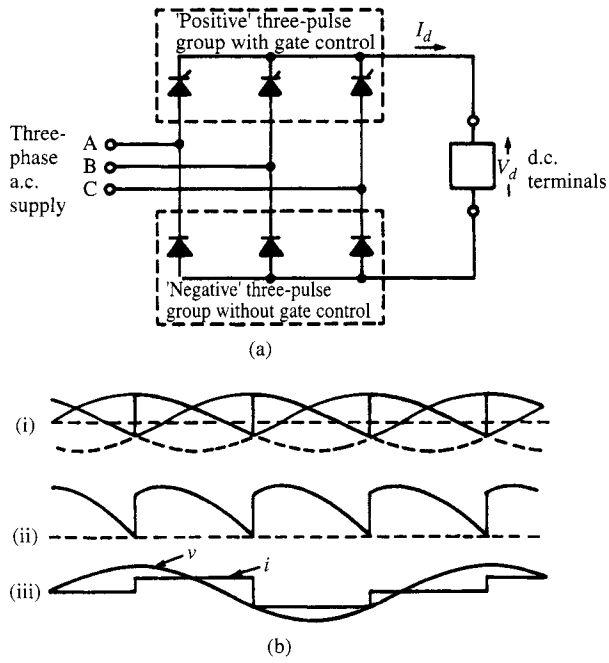

Figure 3.47 (a) Three-phase 'half-controlled' converter and (b) theoretical waveforms for $\alpha = 60$. Trace (i) shows the voltage of a 'positive' group at the d.c. terminal with respect to the supply neutral (———) and the voltage of a 'negative' group at the d.c. terminal with respect to the supply neutral (- - - -). Trace (ii) shows the d.c. terminal voltage of the bridge. Trace (iii) shows the supply voltage and current of phase A

(2) The d.c. current may be modulated from another converter station in the case of a rectifier-inverter link.

(3) The firing angle control systems often given rise to substantial errors in their implementation.

As a result the large static converters often produce harmonic orders and magnitudes not predicted by the Fourier series of the idealised waveforms.

The uncertain nature of these 'uncharacteristic' harmonics makes it difficult to prevent them at the design stage. Filters are not normally provided for uncharacteristic harmonics and as a result their presence often causes more problems than the characteristic harmonics.

By way of example, Table 3.3 shows the results of harmonic measurements during back-to-back testing of the New Zealand d.c. converter station at Benmore. All the harmonic voltages are unbalanced, particularly the third and ninth. The table also illustrates the presence of all current harmonic orders, odd and even, with the uncharacteristic orders causing higher voltage distortion than the characteristic ones. A realistic quantitative analysis of the uncharacteristic harmonic components can only be achieved by a complete three-phase computer model of the system behaviour with detailed representation of the converter controls. A mostly qualitative assessment of the main problem

Table 3.3 Harmonic measurements during back-to-back testing of the New Zealand high voltage d.c. converters

Harmonic	400 A d.c. (one-third full load) current; phase-to-neutral voltages at Benmore on 220 kV		
	Red phase (%)	Yellow phase (%)	Blue phase (%)
1	100	100	100
2	0.5	0.7	1.0
3	2.9	0.3	1.0
4	0.6	0.3	0.4
5	0.25	0.15	0.25
6	0.25	0.30	0.35
7	0.15	0.15	0.1
8	0	0.05	0.1
9	0.05	0.05	0.15
10	0.05	0.05	0.05
11	0.1	0.15	0.1
12	0.15	0.05	0.15
13	0.05	0.05	0.05
14	0.05	0.05	0.05
15	0.15	0	0.2
16	0	0.1	0.15
17	0.3	0.3	0.3
18	0	0.05	0.1
19	0.3	0.3	0.7
20	–	–	–
21	–	–	–
22	0.2	0.2	0.5
23	0.4	0.2	0.3
24	0.2	0.2	0.15

areas and the sensitivity of the system to small deviations from the ideal conditions are considered in this section.

Imperfect a.c. Source Deviations from the perfectly balanced sinusoidal supply can be caused by (i) presence of negative sequence fundamental frequency in the commutating voltage; (ii) harmonic voltage distortion of positive or negative sequence; and (iii) asymmetries in the commutation reactances. In general an imperfect a.c. source produces asymmetrical firing references and d.c. current modulation. The first problem can be eliminated by using equidistant firing control but the second problem still remains. This effect, illustrated in Figure 3.48 for the case of an unrealistically high level of fundamental voltages asymmetry, produces considerable second harmonic content on the d.c. side and third harmonic on the a.c. side [12].

Under normal operating conditions the expected levels of asymmetry and distortion are small and their effects can be approximated with reasonable accuracy.